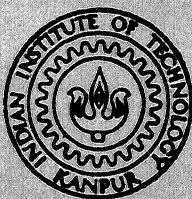# CONJUGATE HEAT TRANSFER IN THE LAMINAR FLOW OF HIGH PRANDTL NUMBER FLUIDS IN A CIRCULAR TUBE SUBJECTED TO NON-UNIFORM CIRCUMFERENTIAL RADIATION HEAT FLUX FROM A LARGE HEATED WALL

by

ALAKANANDA BANDYOPADHYAY

DEPARTMENT OF MECHANICAL ENGINEERING

INDIAN INSTITUTE OF TECHNOLOGY, KANPUR

FEBRUARY, 1987

# CONJUGATE HEAT TRANSFER IN THE LAMINAR FLOW OF HIGH PRANDTL NUMBER FLUIDS IN A CIRCULAR TUBE SUBJECTED TO NON-UNIFORM CIRCUMFERENTIAL RADIATION HEAT FLUX FROM A LARGE HEATED WALL

A Thesis Submitted
In Partial Fulfilment of the Requirements
for the Degree of

## MASTER OF TECHNOLOGY

by

ALAKANANDA BANDYOPADHYAY

*to the*

DEPARTMENT OF MECHANICAL ENGINEERING

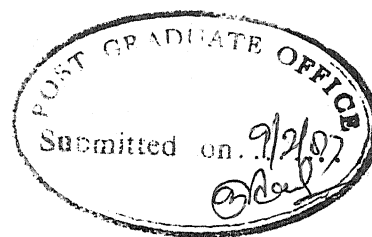INDIAN INSTITUTE OF TECHNOLOGY, KANPUR

FEBRUARY, 1987

ME-1987-M- BAN-CON

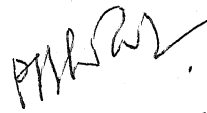*In*

*Loving Memory of*

*My Father*

## CERTIFICATE

This is to certify that the work presented in this thesis entitled "CONJUGATE HEAT TRANSFER IN THE LAMINAR FLOW OF HIGH PRANDTL NUMBER FLUIDS IN A CIRCULAR TUBE SUBJECTED TO NON-UNIFORM CIRCUMFERENTIAL RADIATION HEAT FLUX FROM A LARGE HEATED WALL" has been carried out by Mr. Alakananda Bandyopadhyay under my supervision and has not been submitted elsewhere for a degree.

Dr. P.S. Ghoshdastidar
Assistant Professor
Department of Mechanical Engineering
Indian Institute of Technology
Kanpur

February 1987

## <u>ACKNOWLEDGEMENTS</u>

# CONTENTS

## LIST OF FIGURES

# NOMENCLATURE

Symbols:

C    =    specific heat of the fluid

d    =    vertical distance of the tube from the heated wall (Figure 1(a))

F    =    configuration factor

h    =    convective heat transfer coefficient at the solid-fluid interface

k    =    thermal conductivity

L    =    horizontal distance of the centre of the tube from the left end of the heated wall (Figure 1(a))

N    =    total number of grid points

Nu    =    Nusselt number

Pr    =    Prandtl number

q    =    heat flux

r    =    radial coordinate

$\Delta r$    =    step size in r-direction

Re    =    Reynolds number

T    =    temperature

Th    =    thickness of the tube wall

u    =    axial velocity of the fluid

W    =    width of the heated wall (Figure 1(a))

x    =    axial distance

$\Delta x$    =    step size in x-direction

Greek letters:

$\alpha$    =    thermal diffusivity of the fluid

$\varepsilon$    =    emissivity of the tube material

$\mu$    =    coefficient of viscosity of the fluid

$\nu$ = coefficient of kinematic viscosity of the fluid

$\rho$ = density of the fluid

$\sigma$ = Stefan-Boltzmann constant

$\emptyset$ = circumferential coordinate

$\Delta\emptyset$ = step size in $\emptyset$-direction

Subscripts:

fb = fluid bulk

e = at the entrance of the tube

f = fluid

i = index notation for a node in r-direction

j = index notation for a node in $\emptyset$-direction

k = index notation for a grid in x-direction

P = value at previous x-station

p = at constant pressure

r = along r-direction, entirely in the fluid and wall of the tube

rf = along r-direction, only in fluid region

S = surrounding medium

s = solid

W = heated wall

x = local value

Superscripts:

— = average value

* = non-dimensional value

n = value at the previous iteration.

# ABSTRACT

A simple but computationally efficient finite difference scheme has been used to solve the problem of conjugate heat transfer in a laminar flow of high Prandtl number fluid in a circular tube whose periphery is exposed to non-uniform radiation heat flux from a large heated wall. The present model is a simulation of the effect of hot refractory wall close to a tube in a pipe still.

The results indicate that in a thin tube with low conductivity, the temperature of the tube is very high which may result in hot spots on the tube surface. If the tube material is thick and has a sufficiently high conductivity, the peripheral conduction in the tube wall alleviates this problem. Also, the temperature of the tube goes up when the tube is placed closer to the heated wall.

For the wider wall the mean temperature of the inner wall of the tube is more as the tube receives more radiation. Also, it is observed that mean tube inner wall temperature increases with the axial distance and is lower for higher Prandtl number fluid.

It is also seen that thermal entry lengths are higher for higher Prandtl number fluid and for higher Reynolds number of the flow.

The fluid bulk temperature increases with the axial distance and for higher Prandtl number of the fluid and lower Reynolds number of the flow, the fluid bulk temperatures are less.

The accuracy of the present numerical solution has been checked by comparing it with the analytical solution of the case of fully developed constant heat flux condition on the periphery of a very thin tube. The result is found to be very satisfactory.

# CHAPTER 1

## INTRODUCTION

### 1.1 General

This investigation presents the case of heating of a
fluid flowing through a long circular tube which is exposed to
a non-uniform radiation heat flux on its periphery by the proxi-
mity of a very large heated wall situated parallely above the
axis of the tube. The temperature of the fluid is uniform at
the inlet of the tube where the heat transfer begins, but the
velocity profile is already fully developed and invariant.
This, however, limits the applicability of the present analysis
to fluids whose Prandtl numbers are very high relative to 1,
for example, oils. The present analysis is for constant
property fluids but variable property fluids can also be inves-
tigated with little modification in the solution procedure.

The present model is a simulation of the effect of hot
refractory wall close to a tube in a pipe still. Frequently,
in the case of uneven distribution of heat flux around the
tube, hot spots on the tube surface may occur. If the tube
material is thick and has a sufficiently high conductivity,
peripheral conduction in the wall may alleviate.this problem,
but for thin walled tubes, the difficulty can be accute.

The temperature distribution in the wall is a strong
function of the amount of radiation heat flux received at the
outer surface of the tube and the heat transfer at the interface

between the inner surface of the tube and the fluid. Thus, the conjugate heat transfer at the interface plays an important role in this problem.

## 1.2 Objective

The objectives of the present investigation are (a) to find the temperature distribution in the wall of the tube for various thickness and thermal conductivity of the tube and for various positions of the tube with respect to the heated wall, (b) to get a qualitative indication of the thermal entry lengths for fluids of different Prandtl numbers and for various Reynolds number of the flow, and (c) to show circumferential variation of solid-fluid interface temperatures for different widths of the heated wall.

## 1.3 Literature Survey

The problem of laminar flow in a circular tube with fully developed constant heat rate conditions axially, but with an arbitrary peripheral variation of heat flux, has been treated by Reynolds [1, 2]. In [1], a solution is obtained for a pulse of heat transferred across an elemental section of wall, and superposition is employed to obtain solutions for any prescribed heat flux. In [2], the prescribed heat flux is expressed in terms of a Fourier expansion and also the flow is turbulent. An interesting conclusion of [2] is that the effects of circumferential heat flux variation in turbulent flow are sometimes more pronounced than in laminar flow. The coupled effect of wall and fluid conduction in laminar pipe flow has been studied

by Faghri and Sparrow [3] and Zariffch et al [4] using finite
difference and by Campo and Rangel [5] analytically. Davis
and Venkatesh [6] also studied heat transfer to Poiseuille
flow in a pipe with heat conducting section, as an example of
their new general formulation of the solution of conjugate
boundary value problem. Computations, however, were not per-
formed. Luikov et al [7] presented a closed form analytical
solution for the conjugate heat transfer problem in case of
fluid flow in circular tube. S.V. Patankar [8] suggested the
use of harmonic mean of the transport properties on both sides
of an interface to treat the points of discontinuity. Therm-
ally fully developed flow in a square duct with finite wall
thickness was presented as an example. The method is quite
general and can also calculate fluid flow and heat transfer in
arbitrary geometries. Barozzi and Pagiliarini [9] have used
finite element method to solve axi-symmetric conjugate heat
transfer in a pipe with uniform heat flux specified on its
periphery. The method combines a finite element treatment of
the energy equation in the tube wall and the application of the
Duhamel's theorem at the interface.

## 1.4 Salient Features of the Present Investigation

The present investigation differs from the previous
works on the following counts:

(i)     the non-uniform peripheral heat flux on the outer
        surface of the tube is actually calculated, instead
        of being prescribed.

(ii)    the flow is thermally undeveloped.

(iii)    the problem is non-axisymmetric.

(iv)    a simple but computationally efficient finite difference scheme has been used to solve the problem.

(v)    it has the capability of handling variable property fluid and tube material with little modification in the numerical method.

# CHAPTER 2

## PROBLEM FORMULATION

### 2.1 Description of the Problem

The physical model is depicted in Figure 1(a) and
Figure 1(b). The refractory wall has a width W. The pipe,
which has inside and outside radii $r_1$ and $r_2$, is separated by
a distance d vertically from the wall, the tube being at a
distance L from the left extreme point of the wall. L and d
together determine the position of the tube with respect to
the wall. The wall behaves as a black body radiator at temper-
ature $T_W$. The surrounding is at temperature $T_S$. The upper
portion of the periphery of the tube receives radiation heat
flux both from the wall and the surroundings while the bottom
portion receives radiation heat flux primarily from the surr-
oundings. So, there is non-uniform radiation heat flux on the
periphery of the tube (Figure 1(a)), but the radiation heat flux
is uniform in the axial direction since both the wall and the
tube are very long in that direction (Figure 1(b)). A fluid
enters the tube at a uniform inlet temperature $T_e$ while the
velocity profile is fully developed.

So, the thermal boundary layer develops along the
axis of the tube until the temperature profile is fully deve-
loped. The local heat flux density at any x position from the
inner pipe wall to the fluid is,

$$q_1 = q_1(\emptyset) = h(T_1 - T_{fb})$$

where $T_{fb}$ is the fluid bulk temperature at that x-position
and h is the heat transfer coefficient at the given x (the
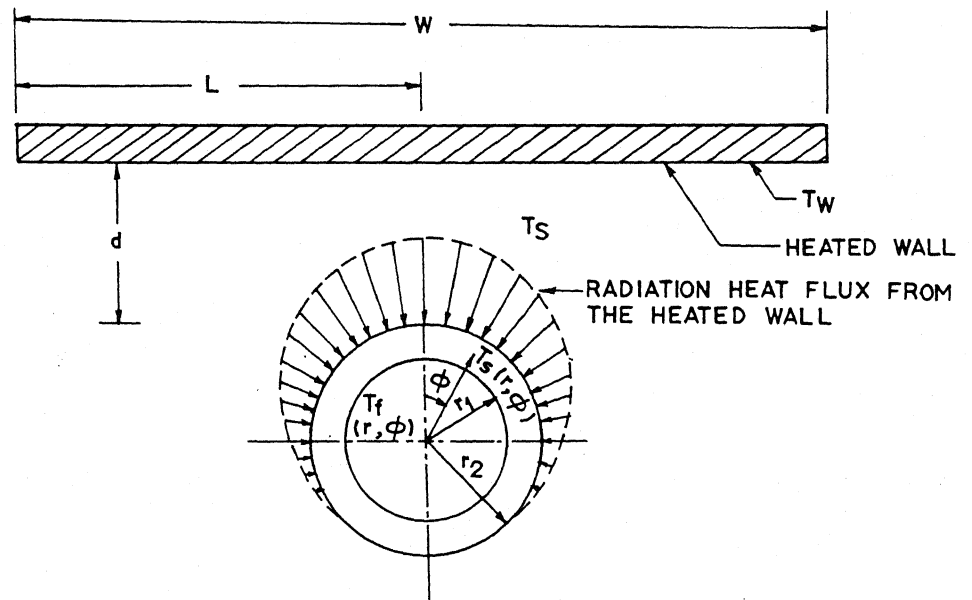
FIG. 1(a) SCHEMATIC DIAGRAM OF THE PROBLEM AND THE
COORDINATE SYSTEM IN (r,φ) DIRECTION
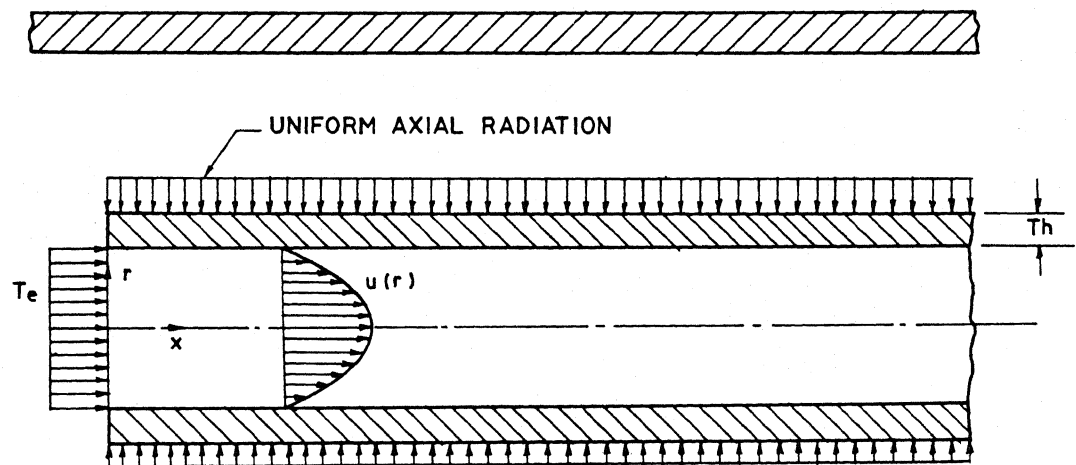


FIG. 1(b) SCHEMATIC DIAGRAM OF THE PROBLEM AND THE
COORDINATE SYSTEM IN (r,x) DIRECTION

method of determination of their values shown later). $T_1$ is the wall temperature at same x-station. The polar coordinates (r, $\emptyset$) are shown in Figure 1(a).

The corresponding radiant flux density to a point on the outer surface where the temperature $T_2 = T_2(\emptyset)$ is,

$$q_2 = q_2(\emptyset) = \sigma\epsilon[F_{2W}(T_W^4 - T_2^4) + (1 - F_{2W})(T_S^4 - T_2^4)]$$

The geometric view factor $F_{2W} = F_{2W}(\emptyset)$ is the fraction of radiation leaving a small area on the outer pipe surface that is directly intercepted by the wall; and the remaining fraction, $1 - F_{2W}$ is absorbed by the remainder of the surroundings. It is described in details in Appendix A.

The temperature distribution in the wall of the tube and the fluid at a particular x-location are determined by solving simultaneously the energy equation in the wall and the fluid and the interface and then the solution marches in the x-direction.

Following assumptions are made to model the problem mathematically:

(a)  The heated wall behaves as a black body radiator.

(b)  The surrounding atmosphere is transparent to thermal radiation.

(c)  Natural convection from the heated wall to the tube surface is neglected, radiation being the principal heat transfer mode.

(d)  The flow is steady, laminar and incompressible.

(e)  Physical properties of both the fluid and the tube wall are constant.

(f)    The tube is smooth so that frictional loss is negligible.

(g)    Axial conduction in the fluid is neglected as in the present case RePr is greater than 100.

(h)    Axial conduction in the tube wall is neglected as the tube is sufficiently long.

(i)    Viscous dissipation is neglected as it is a low speed flow.

## 2.2 Basic Equations

For incompressible, constant property fluid, the combined momentum and continuity equation for fully developed flow becomes,

$$\frac{1}{r} \frac{d}{dr} \left( r \frac{du}{dr} \right) - \frac{1}{\mu} \frac{dp}{dx} = 0$$

with the boundary conditions,

(i)    no slip condition, $u = 0$ at $r = r_1$

(ii)   the velocity is maximum at the centre i.e. $\frac{du}{dr} = 0$ at $r = 0$.

Solving the momentum equation subject to the above boundary conditions, the velocity profile obtained as follows:

$$u(r) = -\frac{1}{4\mu} \frac{dp}{dx} \left[ r_1^2 - r^2 \right]$$

$$\bar{u} = \text{Average velocity (axial)}$$

$$= \frac{u_{max}}{2} = -\frac{1}{8\mu} \frac{dp}{dx} r_1^2$$

as,      $$u_{max} = u(r = 0) = -\frac{1}{4\mu} \frac{dp}{dx} r_1^2$$

Inserting $\bar{u}$ in the expression of $u(r)$, the velocity profile gets the form

$$u(r) = 2\bar{u}\, u^*(r) \qquad (2.1)$$

where $\qquad u^*(r) = 1 - \left(\frac{r}{r_1}\right)^2 \qquad (2.2)$

Energy equations:

(i) For solid region; $\dfrac{\partial^2 T}{\partial r^2} + \dfrac{1}{r}\dfrac{\partial T}{\partial r} + \dfrac{1}{r^2}\dfrac{\partial^2 T}{\partial \phi^2} = 0 \qquad (2.3)$

with boundary conditions,

at $r = r_2$, $\quad -k_s \dfrac{\partial T}{\partial r} = -q_2(\phi) =$ radiation heat

flux falling on the upper surface

$$\therefore \; \frac{\partial T}{\partial r} = \frac{1}{k_s} q_2(\phi) = \frac{\sigma\varepsilon}{k_s}\left[F_{2W}(\phi)(T_W^4 - T_2^4) + \{1 - F_{2W}(\phi)\}(T_S^4 - T_2^4)\right]$$

$$\therefore \; \text{at } r = r_2, \quad \frac{\partial T}{\partial r} = \frac{\sigma\varepsilon}{k_s}\left[F_{2W} T_W^4 + (1 - F_{2W})T_S^4 - T_2^4\right] \qquad (2.3a)$$

where $F_{2W} = F_{2W}(\phi) =$ configuration factor, determined by Hottel-Cross-string method (see Appendix A)

$$T_2 = T\big|_{r=r_2} = T(\phi)$$

(ii) Fluid region;

Energy equation; $\quad u\dfrac{\partial T}{\partial x} = \alpha_f\left[\dfrac{\partial^2 T}{\partial r^2} + \dfrac{1}{r}\dfrac{\partial T}{\partial r} + \dfrac{1}{r^2}\dfrac{\partial^2 T}{\partial \phi^2}\right]$

$$(2.4)$$

with boundary conditions, at $r = 0$, $\dfrac{\partial T}{\partial r} = 0$ $\left.\begin{array}{c}\\ \\ \end{array}\right\}$

at $x = 0$, $T = T_e$ $\qquad (2.4a)$

At the interface, the equality of temperature and heat flux exists, so that,

at $r = r_1$, $T|_s = T|_f$

$$\text{and} \quad -k_s \left.\frac{\partial T}{\partial r}\right|_s = -k_f \left.\frac{\partial T}{\partial r}\right|_f$$

(2.5)

## 2.3 Fluid Bulk Temperature

For the calculation of the convective heat transfer coefficient h(x) from the wall to the fluid along the axis of the tube (x-direction), it is necessary to define a characteristic temperature of the fluid commonly known as 'bulk temperature' or 'mixing cup temperature'. The reason is that in a tube flow there is no easily discernible free-stream condition as is present in the flow over a flat plate. For most tube or channel flow heat transfer problems the topic of central interest is the total energy transferred to the fluid in either an elemental length of the tube or over the entire length of the channel. At any x position, the temperature that is indicative of the total energy of the flow is an integrated mass-energy average temperature over the entire flow area. The numerator of equation (2.6) below, represents the total energy flow through the tube and the denominator of the same equation represents the product of mass flow and specific heat integrated over the flow area. The bulk temperature is thus representative of the total energy of the flow at a particular location.(x).

Mathematically the bulk temperature for the fluid is defined as,

$$T_{fb} = \frac{\int_o^{2\pi} \int_o^{r_1} \rho\, C_p\, u\, T\, r\, dr\, d\emptyset}{\int_o^{2\pi} \int_o^{r_1} \rho\, C_p\, u\, r\, dr\, d\emptyset} \qquad (2.6)$$

Thus

$$T_{fb} = T_{fb}(x)$$

The heat flux from the wall of the tube to the fluid at a given x-location and circumferential location $\emptyset$, $q_1(x, \emptyset)$ is defined as,

$$q_1(x, \emptyset) = -[- k_s \left.\frac{\partial T}{\partial r}\right|_{r=r_1, s}] = k_s \left.\frac{\partial T}{\partial r}\right|_{r=r_1, s} \qquad (2.7)$$

and the average heat flux at a given x is defined as,

$$\bar{q}_1(x) = \frac{1}{2\pi} \int_o^{2\pi} q_1\, d\emptyset \qquad (2.7a)$$

The average wall temperature of the tube at a given x is expressed as,

$$\bar{T}_1(x) = \frac{1}{2\pi} \int_o^{2\pi} T_1\, d\emptyset \qquad (2.8)$$

where $T_1 = T_1(x, \emptyset)$ = Interface temperature = $T|_{r=r_1}$ (2.8a)

Local heat transfer coefficient, $h_x$ can be found by the following heat flux balance equation;

$$\bar{q}_1(x) = h_x(\bar{T}_1 - T_{fb})$$

or, $$h_x = \frac{\bar{q}_1(x)}{\bar{T}_1 - T_{fb}} \qquad (2.9)$$

The local Nusselt number, $Nu_x$ is found by,

$$Nu_x = \frac{h_x(2r_1)}{k_f}$$

(2.10)

CHAPTER 3

METHOD OF SOLUTION

## 3.1 Finite Difference Approximations

The energy equations of the solid and the fluid along with the compatibility conditions at the interface are discretised using finite difference approximations as described below.

A typical orthogonal mesh system for using the Finite Difference approximation is shown in Figure 2.

The following finite difference approximations are used.

(i) Using central difference formulae for the terms $\frac{\partial^2 T}{\partial r^2}$, $\frac{\partial T}{\partial r}$ and $\frac{\partial^2 T}{\partial \phi^2}$ at the point $(i, j)$,

$$\frac{\partial^2 T}{\partial r^2} = \frac{1}{(\Delta r)^2} [T_{i+1,j} - 2T_{i,j} + T_{i-1,j}]$$

$$\frac{\partial^2 T}{\partial \phi^2} = \frac{1}{(\Delta \phi)^2} [T_{i,j+1} - 2T_{i,j} + T_{i,j-1}]$$

$$\frac{\partial T}{\partial r} = \frac{1}{2(\Delta r)} [T_{i+1,j} - T_{i-1,j}]$$

where  $\Delta r$ = uniform step size in r-direction

$\Delta \phi$ = uniform step size in $\phi$-direction

i  = index in r-direction

j  = index in $\phi$-direction.

(ii) Using backward difference formula for the convection term $\frac{\partial T}{\partial x}$ at a x-station, k+1,

$$\frac{\partial T}{\partial x} = \frac{T_{i,j,k+1} - T_{i,j,k}}{\Delta x}$$
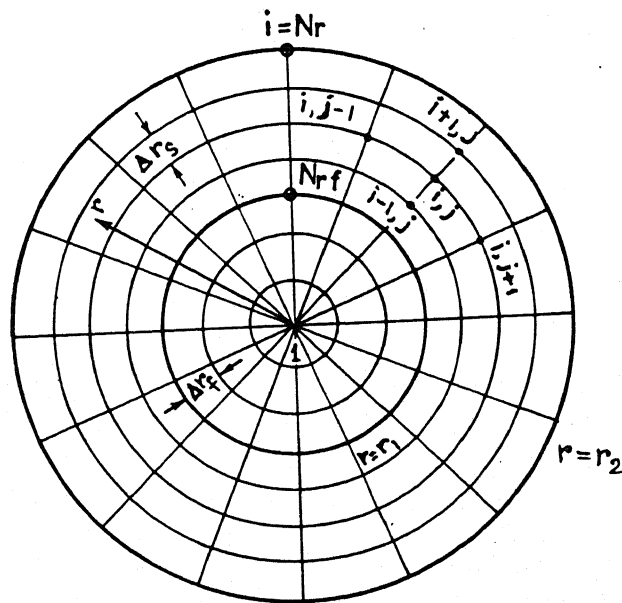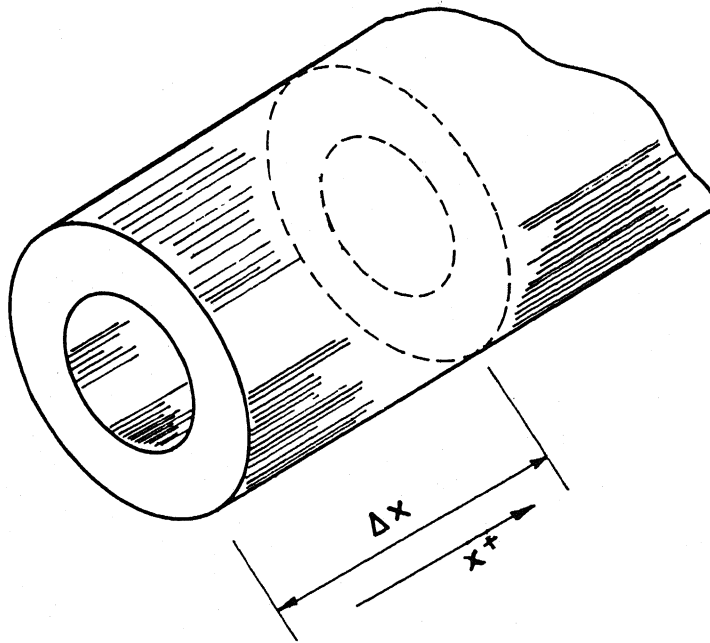
FIG. 2 A TYPICAL FINITE DIFFERENCE GRID SYSTEM FOR THE PROBLEM

where $T_{i,j,k}$ = Temperature of the point (i, j) at the previous x-station.

Also $\frac{\partial T}{\partial r}$ term can be discretised by backward difference formula as,

$$\frac{\partial T}{\partial r}\bigg|_{i+1,j} = \frac{T_{i+1,j} - T_{i,j}}{\Delta r}$$

## 3.1.1 Discretization of the Energy Equation for Solid

The equation (2.3) subjected to the boundary condition (2.3a) can be discretized as follows,

Equation (2.3); $\quad \frac{\partial^2 T}{\partial r^2} + \frac{1}{r}\frac{\partial T}{\partial r} + \frac{1}{r^2}\frac{\partial^2 T}{\partial \phi^2} = 0$

Boundary condition (2.3a); at $r = r_2$;

$$\frac{\partial T}{\partial r} = \frac{\sigma \varepsilon}{k_s}[F_{2W} T_W^4 + (1 - F_{2W})T_S^4 - T_2^4]$$

Refer to Figure 2.

Let, $N_r$ = Number of grid points in r-direction for the entire fluid-solid region

$N_\phi$ = Number of grid points in $\phi$-direction, both for solid and fluid region

$N_{rf}$ = Number of grid points in r-direction, only in the fluid region.

As x-direction is taken infinitely long, no specific number of grid points are taken for this direction. By marching procedure the solution can be continued upto any length and it can be terminated as per requirement.

The uniform step sizes are,

$$\Delta r_s = \frac{(r_2 - r_1)}{(N_r - N_{rf})}$$

$$\Delta \emptyset = \frac{2\pi}{N_\emptyset}$$

and $\quad \Delta r_f = \dfrac{r_1}{(N_{rf} - 1)}$

Discretizing equation (2.3) by finite difference approximation, as

$$\frac{1}{(\Delta r_s)^2}[T_{i-1,j} - 2T_{i,j} + T_{i+1,j}] + \frac{1}{r_i}\frac{1}{2\Delta r_s}[T_{i+1,j} - T_{i-1,j}]$$

$$+ \frac{1}{r_i^2}\frac{1}{(\Delta \emptyset)^2}[T_{i,j-1} - 2T_{i,j} + T_{i,j+1}] = 0$$

Simplifying the above equation,

$$(2r_i^2 - r_i \Delta r_s)T_{i-1,j} - [4r_i^2 + 4(\frac{\Delta r_s}{\Delta \emptyset})^2]T_{i,j}$$

$$+ (2r_i^2 + r_i \Delta r_s)T_{i+1,j} = -2(\frac{\Delta r_s}{\Delta \emptyset})^2[T_{i,j-1} + T_{i,j+1}]$$

Writing the above equation in the standard tridiagonal matrix form,

$$A_i T_{i-1,j} + B_i T_{i,j} + C_i T_{i+1,j} = D_i \qquad (3.1)$$

where $\quad A_i = 2r_i^2 - r_i \Delta r_s$

$$B_i = -[4r_i^2 + 4(\frac{\Delta r_s}{\Delta \emptyset})^2]$$

$$C_i = 2r_i^2 + r_i \Delta r_s$$

$$D_i = -2(\frac{\Delta r_s}{\Delta \emptyset})^2[T_{i,j-1} + T_{i,j+1}]$$

The above equation is valid for any interior point (i, j) of the tube wall except the boundary points, i.e. for all nodes numbering from $i = N_{rf} + 1$ to $i = N_r - 1$ and in $\phi$-direction all points except the points at $\phi = 0$ and $\phi = (2\pi - \phi)$ i.e. $j = 1$ and $j = N_\phi$.

More correctly saying, the equation (3.1) is valid also for $j = 1$ and $j = N_\phi$, but for computational purpose the equation is slightly modified for all points with $j = 1$ and $j = N_\phi$, as described below.

For $j = 1$, the point $(j-1)$ physically represents the point '$N_\phi$'. Therefore the equation (3.1) is modified by replacing $(j-1)$ by $N_\phi$ for $j = 1$ and $(j+1)$ by $1$ for $j = N_\phi$, both changes occur in the expression of $D_i$.

Rewriting equation (3.1) for different j's the general form becomes,

$$A_i T_{i-1,j} + B_i T_{i,j} + C_i T_{i+1,j} = D_i \tag{3.1}$$

with
$$A_i = 2r_i^2 - r_i \Delta r_s$$

$$B_i = -[4 r_i^2 + 4(\frac{\Delta r_s}{\Delta \phi})^2] \quad , \text{ for all } j$$

$$C_i = 2r_i^2 + r_i \Delta r_s$$

and
$$D_i = -2(\frac{\Delta r_s}{\Delta \phi})^2 [T_{i,j-1} + T_{i,j+1}] \quad \text{for } 2 \leq j \leq (N_\phi - 1)$$

$$= -2(\frac{\Delta r_s}{\Delta \phi})^2 [T_{i,N_\phi} + T_{i,2}] \quad \text{for } j = 1$$

$$= -2(\frac{\Delta r_s}{\Delta \phi})^2 [T_{i,1} + T_{i,N_\phi-1}] \quad \text{for } j = N_\phi$$

However the equation (3.1) is only valid for interior points of the tube wall.

To get the discretised energy equation for the upper surface, i.e. $i = N_r$ $(r = r_2)$, the boundary condition (2.3a) is used to modify equation (3.1) as described below.

Boundary condition (2.3a) is, at $r = r_2$ (i.e. $i = N_r$),

$$\frac{\partial T}{\partial r} = \frac{\sigma \epsilon}{k_s} [F_{2W} T_W^4 + (1 - F_{2W}) T_S^4 - T_2^4]$$

where $T_2$ = temperature of the tube at $r = r_2$, this is represented by T.

Putting T in place of $T_2$ and discretising equation (2.3a)

$$\frac{T_{i+1,j} - T_{i-1,j}}{2 \Delta r_s} = \frac{\sigma \epsilon}{k_s} [F_{2W_j} T_W^4 + (1 - F_{2W_j}) T_S^4 - T_{i,j}^4]$$

but as $T_{i,j}^4$ term introduces non-linearity in the discretized equation it is necessary to linearize this term using Patankar's approach [10] to linearization of the source term.

According to this approach, the non-linear term should be linearized in such a manner so that fast convergence is attained. It also suggests that when the coefficient of the transformed linear term is equal to the slope of the original nonlinear term the convergence is fastest, however this is not true always.

Using this approach $T_{i,j}^4$ term is linearized as,

$$T_{i,j}^4 = 4(T_{i,j}^n)^3 T_{i,j} - 3(T_{i,j}^n)^4$$

where $T_{i,j}^n$ = Temperature at point (i, j) in the previous iteration.

Putting this in the discretized equation of the boundary condition (2.3a), the equation becomes,

$$\frac{T_{i+1,j} - T_{i-1,j}}{2\Delta r_s} = \frac{\sigma\varepsilon}{k_s}\left[F_{2W_j}T_W^4 + (1 - F_{2W_j})T_S^4 + 3(T_{i,j}^n)^4 - 4(T_{i,j}^n)^3 T_{i,j}\right]$$

Simplifying it,

$$T_{i+1,j} = \frac{2\sigma\varepsilon}{k_s}\Delta r_s\left[F_{2W_j}T_W^4 + (1 - F_{2W_j})T_S^4 + 3(T_{i,j}^n)^4 - 4(T_{i,j}^n)^3 T_{i,j}\right] + T_{i-1,j}$$

Putting this expression in equation (3.1) the discretized energy equation for $i = N_r$ is obtained as follows.

$$A_i T_{i-1,j} + B_i T_{i,j} + C_i T_{i+1,j} = D_i \qquad (3.1a)$$

where 
$$A_i = 4r_i^2 = 4r_2^2 \quad (\text{as } i = N_r \Rightarrow r_i = r_2)$$

$$B_i = -4S_2(T_{i,j}^n)^3 - 4r_2^2 - 4\left(\frac{\Delta r_s}{\Delta\phi}\right)^2$$

$$C_i = 0$$

$$D_i = -2\left(\frac{\Delta r_s}{\Delta\phi}\right)^2 [T_{i,j-1} + T_{i,j+1}]$$
$$- S_2[F_{2W_j}T_W^4 + (1 - F_{2W_j})T_S^4 + 3(T_{i,j}^n)^4]$$

where 
$$S_2 = \frac{2\sigma\varepsilon}{k_s}\Delta r_s(2r_2^2 + r_2\Delta r_s).$$

The above equation is valid for $i = N_r$ only, here also $D_i$ is modified for $j = 1$ and $j = N_\phi$ as before, i.e. replacing $(j-1)$ by $N_\phi$ for $j = 1$ and $(j+1)$ by 1 for $j = N_\phi$.

### 3.1.2 Discretization of the Energy Equation for Fluid

The energy equation for fluid (Equation (2.4)) is changed by inserting the expression of u(r) into it as below.

$$2\bar{u}\ u*(r)\ \frac{\partial T}{\partial x} = \alpha_f\ [\frac{\partial^2 T}{\partial r^2} + \frac{1}{r}\frac{\partial T}{\partial r} + \frac{1}{r^2}\frac{\partial^2 T}{\partial \emptyset^2}]$$

or,

$$\frac{2\bar{u}}{\alpha_f}\ u*(r)\ \frac{\partial T}{\partial x} = \frac{\partial^2 T}{\partial r^2} + \frac{1}{r}\frac{\partial T}{\partial r} + \frac{1}{r^2}\frac{\partial^2 T}{\partial \emptyset^2}$$

Discretizing this equation using finite difference approximation for any point (i, j) in the fluid region and at a x-station (k+1),

$$\frac{2\bar{u}\ u_i^*}{\alpha_f} \cdot \frac{T_{i,j,k+1} - T_{i,j,k}}{\Delta x} = \frac{1}{(\Delta r_f)^2}[T_{i-1,j} - 2T_{i,j} + T_{i,j+1}]_{k+1}$$

$$+ \frac{1}{r_i}\ \frac{1}{2\Delta r_f}[T_{i+1,j} - T_{i-1,j}]_{k+1} + \frac{1}{r_i^2}\ \frac{1}{(\Delta \emptyset)^2}[T_{i,j-1}$$

$$- 2T_{i,j} + T_{i,j+1}]_{k+1}$$

For simplification the two dimensional notation for T is used, replacing $T_{i,j,k}$ by $T_{P_{i,j}}$ and $T_{i,j,k+1}$ by $T_{i,j}$.

Simplifying the above discretized energy equation for fluid and writing it in the standard form of tri-diagonal matrix, as below,

$$A_i T_{i-1,j} + B_i T_{i,j} + C_i T_{i+1,j} = D_i \qquad (3.2a)$$

where $A_i = 2r_i^2 - \Delta r_f\ r_i$

$$B_i = -[4\ r_i^2 + 4(\frac{\Delta r_f}{\Delta \emptyset})^2 + C\ r_i^2\ u_i^*]$$

$$C_i = 2r_i^2 + \Delta r_f \, r_i$$

$$D_i = -2\left(\frac{\Delta r_f}{\Delta \emptyset}\right)^2 [T_{i,j-1} + T_{i,j+1}] - C \, u_i^* \, r_i^2 \, T_{P_{i,j}}$$

where $\quad C = \dfrac{4\bar{u}(\Delta r_f)^2}{\alpha_f \, \Delta x}$

Equation (3.2a) is valid for $i = 2$ to $i = N_{rf} - 1$. As in the case of solid region, this equation is also modified for $j = 1$ and $j = N_\emptyset$ and the modification takes place in the expression of $D_i$.

The boundary condition (2.4a) is discretized as below.

For $i = 1$, i.e. $r = 0$; $\frac{\partial T}{\partial r} = 0$

discretizing it; $\quad \dfrac{T_{2,j} - T_{1,j}}{\Delta r_f} = 0$

or, $\quad\quad\quad -T_{1,j} + T_{2,j} = 0$ $\hfill$ (3.2b)

Combining equations (3.2a) and (3.2b) the general form of the discretized energy equation for fluid is obtained as below,

$$A_i T_{i-1,j} + B_i T_{i,j} + C_i T_{i+1,j} = D_i \hspace{1cm} (3.2)$$

where $\quad A_i = 2r_i^2 - r_i \, \Delta r_f$

$$B_i = -\left[4r_i^2 + 4\left(\frac{\Delta r_f}{\Delta \emptyset}\right)^2 + C \, r_i^2 \, u_i^*\right]$$

$$C_i = 2r_i^2 + r_i \, \Delta r_f$$

$$D_i = -2\left(\frac{\Delta r_f}{\Delta \emptyset}\right)^2 [T_{i,j-1} + T_{i,j+1}] - C \, u_i^* \, r_i^2 \, T_{P_{i,j}}$$

valid for $i = 2$ to $i = N_{rf} - 1$

and also for $i = 1$, $\quad A_i \;=\; 0$

$$B_i \;=\; -1$$

$$C_i \;=\; 1$$

$$D_i \;=\; 0$$

Equation (3.2) is modified for $j = 1$ and $j = N_{\emptyset}$.

### 3.1.3 Discretization of the Compatibility Conditions at the Fluid-Solid Interface

The compatibility conditions (equation (2.5)) are,

at $r = r_1$, $\qquad k_s \left.\dfrac{\partial T}{\partial r}\right|_s \;=\; k_f \left.\dfrac{\partial T}{\partial r}\right|_f$ and $\quad T|_s \;=\; T|_f$

Energy equation for solid, equation (2.3)

$$\frac{\partial^2 T}{\partial r^2} + \frac{1}{r}\frac{\partial T}{\partial r} + \frac{1}{r^2}\frac{\partial^2 T}{\partial \emptyset^2} \;=\; 0$$

and energy equation for fluid, equation (2.4)

$$\frac{2\bar{u}}{\alpha_f}\, u^*(r)\,\frac{\partial T}{\partial x} \;=\; \frac{\partial^2 T}{\partial r^2} + \frac{1}{r}\frac{\partial T}{\partial r} + \frac{1}{r^2}\frac{\partial^2 T}{\partial \emptyset^2}$$

Refer to Figure 3.

From Taylor's series expansion for point $(i-1,j)$,

$$T_{i-1,j} \;=\; T_{i,j} - \Delta r_f\left(\frac{\partial T}{\partial r}\right)_{i,j,f} + \frac{\Delta r_f^2}{2}\left(\frac{\partial^2 T}{\partial r^2}\right)_{i,j,f}$$

Solving $\left(\dfrac{\partial^2 T}{\partial r^2}\right)_{i,j,f}$ from the above equation

$$\left(\frac{\partial^2 T}{\partial r^2}\right)_{i,j,f} \;=\; \frac{2}{(\Delta r_f)^2}\left[T_{i-1,j} - T_{i,j} + \Delta r_f\left(\frac{\partial T}{\partial r}\right)_{i,j,f}\right]$$

At the interface $u_i^* = 0$, also $r_i = r_1$.
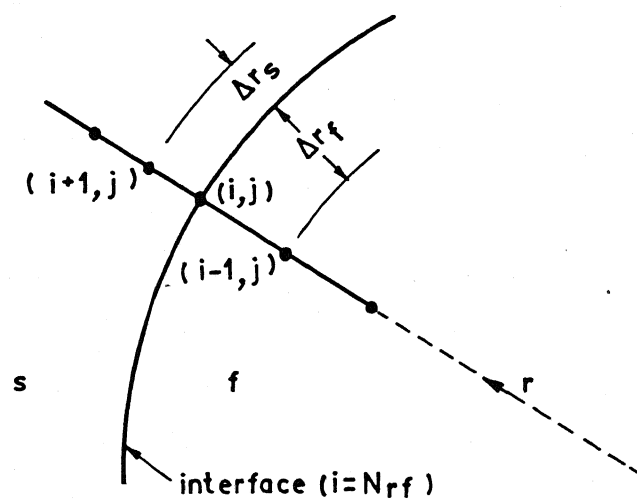
FIG. 3 FINITE DIFFERENCE NODES NEAR THE
INTERFACE

Putting all these in the energy equation for fluid, i.e. in equation (2.4),

$$0 = \frac{2}{(\Delta r_f)^2} [T_{i-1,j} - T_{i,j} + \Delta r_f (\frac{\partial T}{\partial r})_{i,j,f}]$$

$$+ \frac{1}{r_1} (\frac{\partial T}{\partial r})_{i,j,f} + \frac{1}{r_1^2} (\frac{\partial^2 T}{\partial \phi^2})_{i,j,f}$$

Simplifying it,

$$(\frac{\partial T}{\partial r})_{i,j,f} = \frac{2r_1}{2r_1 \Delta r_f + (\Delta r_f)^2} [T_{i,j} - T_{i-1,j} - \frac{(\Delta r_f)^2}{2r_1^2} (\frac{\partial^2 T}{\partial \phi^2})_{i,j,f}] \tag{3.3a}$$

Expressing $T_{i+1,j}$ in Taylor's series as,

$$T_{i+1,j} = T_{i,j} + \Delta r_s (\frac{\partial T}{\partial r})_{i,j,s} + \frac{(\Delta r_s)^2}{2} (\frac{\partial^2 T}{\partial r^2})_{i,j,s}$$

thereby,

$$(\frac{\partial^2 T}{\partial r^2})_{i,j,s} = \frac{2}{(\Delta r_s)^2} [T_{i+1,j} - T_{i,j} - r_s (\frac{\partial T}{\partial r})_{i,j,s}]$$

Using this in the energy equation of solid and simplifying it, the $(\frac{\partial T}{\partial r})_{i,j,s}$ term is expressed as below,

$$(\frac{\partial T}{\partial r})_{i,j,s} = \frac{2r_1}{2r_1 \Delta r_s - (\Delta r_s)^2} [T_{i+1,j} - T_{i,j} - \frac{(\Delta r_s)^2}{2r_1^2} (\frac{\partial^2 T}{\partial \phi^2})_{i,j,s}] \tag{3.3b}$$

Ultimately two expressions are obtained for the temperature gradient at the interface for fluid and solid regions as,

$$(\frac{\partial T}{\partial r})_{i,j,f} = - \frac{2r_1}{\Delta r_f (2r_1 + \Delta r_f)} [T_{i-1,j} - T_{i,j} + \frac{(\Delta r_f)^2}{2r_1^2} (\frac{\partial^2 T}{\partial \phi^2})_{i,j,f}]$$

and

$$\left(\frac{\partial T}{\partial r}\right)_{i,j,s} = \frac{2r_1}{\Delta r_s(2r_1 - \Delta r_s)}\left[T_{i+1,j} - T_{i,j} + \frac{(\Delta r_s)^2}{2r_1^2}\left(\frac{\partial^2 T}{\partial \phi^2}\right)_{i,j,s}\right]$$

The compatibility conditions (equation (2.5)), i.e. $T|_s = T|_f$

at $r = r_1$ and

$$k_s \left.\frac{\partial T}{\partial r}\right|_s = k_f \left.\frac{\partial T}{\partial r}\right|_f \quad \text{at} \quad r = r_1$$

$\left(\frac{\partial^2 T}{\partial \phi^2}\right)_{i,j,f}$ and $\left(\frac{\partial^2 T}{\partial \phi^2}\right)_{i,j,s}$ will be equal and both of them have same expression because the temperature of fluid and solid are the same at the interface and $\frac{\partial^2 T}{\partial \phi^2}$ is expressed as,

$$\left(\frac{\partial^2 T}{\partial \phi^2}\right)_{i,j,s} = \left(\frac{\partial^2 T}{\partial \phi^2}\right)_{i,j,f} = \left(\frac{\partial^2 T}{\partial \phi^2}\right)_{i,j,r=r_1}$$

$$= \frac{T_{i,j-1} - 2T_{i,j} + T_{i,j+1}}{(\Delta \phi)^2}$$

Using the heat flux equality condition, i.e.

$$k_s\left(\frac{\partial T}{\partial r}\right)_{i,j,s} = k_f\left(\frac{\partial T}{\partial r}\right)_{i,j,f}$$

and expressing $\left(\frac{\partial T}{\partial r}\right)_{i,j,s}$ and $\left(\frac{\partial T}{\partial r}\right)_{i,j,f}$ as in equations (3.3a) and (3.3b), the following equation is resulted

$$\frac{k_s}{k_f} \cdot \frac{2r_1}{2r_1 \Delta r_s - (\Delta r_s)^2}\left[T_{i+1,j} - T_{i,j} + \frac{(\Delta r_s)^2}{2r_1^2}\left(\frac{\partial^2 T}{\partial \phi^2}\right)_{i,j}\right]$$

$$= \frac{2r_1}{2r_1 \Delta r_f + (\Delta r_f)^2}\left[T_{i,j} - T_{i-1,j} - \frac{(\Delta r_f)^2}{2r_1^2}\left(\frac{\partial^2 T}{\partial \phi^2}\right)_{i,j}\right]$$

Using the expression of $\left(\frac{\partial^2 T}{\partial \phi^2}\right)_{i,j}$ in the above equation and after necessary simplifications the standard discretized equation for the interface is obtained as below,

$$A_i T_{i-1,j} + B_i T_{i,j} + C_i T_{i+1,j} = D_i \quad \text{(for } i = N_{rf}\text{)}$$

$$(3.3)$$

where, $A_i = 2r_1^2 = C_i$

$$B_i = -(2r_1^2 R + 2r_1^2 + RR)$$

$$D_i = -RR(T_{i,j+1} + T_{i,j-1})$$

where $R = \dfrac{k_s}{k_f} \cdot \dfrac{2r_1 \Delta r_f + (\Delta r_f)^2}{2r_1 \Delta r_s - (\Delta r_s)^2}$

and $RR = \dfrac{R(\Delta r_s)^2 + (\Delta r_f)^2}{(\Delta \emptyset)^2}$

Equation (3.3) is valid for all j's except $j = 1$ and $j = N_\emptyset$. For these two j-stations the equation is modified by replacing (j-1) by $N_\emptyset$ for $j = 1$ and (j+1) by 1 for $j = N_\emptyset$.

### 3.1.4 Simplified Equations for $T_{fb}$ and $q_1(x, \emptyset)$

From equation (2.6), $T_{fb} = \dfrac{\int_0^{2\pi} \int_0^{r_1} u\, T\, r\, dr\, d\emptyset}{\int_0^{2\pi} \int_0^{r_1} u\, r\, dr\, d\emptyset}$, as

$\rho C_p$ = Constant for the fluid.

Putting the expression of $u(r) = 2\bar{u} \cdot u^*(r)$, where $u^*(r) = 1 - (\dfrac{r}{r_1})^2$, then simplifying the above expression for $T_{fb}$ the following expression is obtained,

$$T_{fb} = \dfrac{2}{\pi r_1^2} \int_0^{2\pi} \int_0^{r_1} u^*(r)\, T\, r\, dr\, d\emptyset \qquad (3.4)$$

The heat flux, $q_1(x, \emptyset)$,

$$q_1(x, \emptyset) = k_s \left. \frac{\partial T}{\partial r} \right|_{r=r_1,s} = k_s \frac{T_{N_{rf}+1,j} - T_{N_{rf},j}}{\Delta r_s}$$

$$(3.5)$$

## 3.2  Numerical Solution of the Discretized Equations

The set of discretized equations to be solved are listed below.

Equation (3.2),     $A_i T_{i-1,j} + B_i T_{i,j} + C_i T_{i+1,j} = D_i$

where   $A_i = 2r_i^2 - r_i \Delta r_f$

$$B_i = - \left[ 4r_i^2 + 4\left(\frac{\Delta r_f}{\Delta \emptyset}\right)^2 + C \, r_i^2 \, u_i^* \right]$$

$$C_i = 2r_i^2 + r_i \Delta r_f$$

$$D_i = - 2\left(\frac{\Delta r_f}{\Delta \emptyset}\right)^2 \left[ T_{i,j-1} + T_{i,j+1} \right] - C \, u_i^* \, r_i^2 \, T_{P_{i,j}}$$

$$\text{for } i = 2 \text{ to } i = N_{rf} - 1$$

and

$$A_i = 0$$
$$B_i = - 1$$
$$C_i = 1 \qquad , \qquad \text{for } i = 1$$
$$D_i = 0$$

Equation (3.3),     $A_i T_{i-1,j} + B_i T_{i,j} + C_i T_{i+1,j} = D_i$

where   $A_i = 2r_1^2 = C_i$

$$B_i = - \left[ 2r_1^2 R + 2r_1^2 + RR \right]$$

$$D_i = -RR(T_{i,j+1} + T_{i,j-1})$$

$$R = \frac{k_s}{k_f} \cdot \frac{2r_1 \Delta r_f + (\Delta r_f)^2}{2r_1 \Delta r_s - (\Delta r_s)^2}$$

and

$$RR = \frac{R(\Delta r_s)^2 + (\Delta r_f)^2}{(\Delta\phi)^2}$$

Equations (3.1) and (3.1a) combinedly written as

$$A_i T_{i-1,j} + B_i T_{i,j} + C_i T_{i+1,j} = D_i \qquad (3.1b)$$

where

$$A_i = 2r_i^2 - r_i \Delta r_s$$

$$B_i = -[4r_i^2 + 4(\frac{\Delta r_s}{\Delta\phi})^2]$$

$$C_i = 2r_i^2 + r_i \Delta r_s$$

for $i = N_{rf} + 1$

to $i = N_r - 1$

$$D_i = -2(\frac{\Delta r_s}{\Delta\phi})^2 [T_{i,j-1} + T_{i,j+1}]$$

and

$$A_i = 3r_2^2$$

$$B_i = -[4S_2(T_{i,j}^n)^3 + 4r_2^2 + 4(\frac{\Delta r_s}{\Delta\phi})^2]$$

$$C_i = 0$$

$$D_i = -2(\frac{\Delta r_s}{\Delta\phi})^2 [T_{i,j-1} + T_{i,j+1}]$$

$$- S_2 [F_{2W_j} T_W^4 + (1 - F_{2W_j})T_S^4 + 3(T_{i,j}^n)^4]$$

where $S_2 = \frac{2\sigma\varepsilon}{k_s} \Delta r_s (2r_2^2 + r_2 \Delta r_s)$, valid for $i = N_r$.

All the above equations are to be modified for $j = 1$ and $j = N_\phi$, the modifications will be only in the expression of $D_i$. For

$j = 1$, $(j-1)$ is to be replaced by $N_\emptyset$ and for $j = N_\emptyset$, $(j+1)$ is substituted by 1.

Equation (3.4), $\quad T_{fb}(x) = \dfrac{2}{\pi r_1^2} \displaystyle\int_0^{2\pi} \int_0^{r_1} u*(r)\, T\, r\, dr\, d\emptyset$

Equation (3.5), $\quad q_1(x, \emptyset) = k_s \dfrac{T_{N_{rf}+1,j} - T_{N_{rf},j}}{r_s}$

Equation (2.7a), $\quad \bar{q}_1(x) = \dfrac{1}{2\pi} \displaystyle\int_0^{2\pi} q_1\, d\emptyset$

Equation (2.8), $\quad \bar{T}_1(x) = \dfrac{1}{2\pi} \displaystyle\int_0^{2\pi} T_1\, d\emptyset$

Equation (2.9), $\quad h_x = \dfrac{\bar{q}_1(x)}{\bar{T}_1 - T_{fb}}$

Equation (2.10), $\quad Nu_x = \dfrac{h_x(2r_1)}{k_f}$

The set of discretized equations (3.2), (3.3) and (3.1b) for fluid, interface and solid are to be solved by a suitable numerical technique.

In the present analysis a line-by-line method, suggested by Patankar [10], is used. The line-by-line method helps to solve the set of simultaneous linear algebraic equations by Tri-Diagonal Matrix Algorithm (TDMA) method.

The line-by-line method is described in Appendix-B in great detail.

## 3.3  Algorithm for the Numerical Solution

To solve the discretized equation (3.2), (3.3) and (3.1b) to get the temperature at a particular x-location, the following steps are taken.

(a)   The computations are stated at the location $x = \Delta x$ using the known inlet temperature at the entrance of the tube.

(b)   The r-direction lines are selected to initiate the solution procedure by line-by-line method.

(c)   All the temperatures are assumed initially, both in the fluid and solid region.

(d)   Start solving by TDMA with the line $\emptyset = 0$. The temperature at all the grids of this line are solved.

(e)   Go to the next line along $\emptyset$-direction (i.e. at $\emptyset = \Delta\emptyset$) and solve the discretized equations to get temperature at all nodes on that line.

(f)   This procedure is followed one after another for all the r-direction lines.

(g)   The steps 'd' to 'f' are repeated till the process converges, i.e. the temperature at any node does not change further with iterative procedure.

After getting the converged values of temperature, they are stored for that particular x-station. Then the fluid bulk temperature, the average heat flux, the local values of convective heat transfer coefficient and the Nusselt number are calculated following the equations (3.4), (3.5) and (2.7a)

to (2.10). The integrations involved are done by Simpson's rule of numerical integration.

The procedure then marches in x-direction and continued till the fully developed situation is reached. The fully developed situation is indicated when there is no considerable change in $Nu_x$ along x.

The accompanying Flow-chart (Fig. 4) represents the algorithm pictorially. The input data to the program and the listing of the computer program are given in Appendix-C and Appendix-D respectively.

( START )

Initialise all the input data to the program

Calculate the configuration factor at different
$\emptyset$-location by calling the subroutine 'CONFIG'

$k \leftarrow 1$

Guess the temperature of all nodes in $(r, \emptyset)$
direction at this x-location to initiate the
iterative process

Solve the temperature of all nodes in r-direction
at $\emptyset = 0^\circ$ by calling subroutine 'TRIDAG' and in
this way all the '$\emptyset$-constant' lines are solved

Does
the iterative
process converge
?
— No → Continue
iterations

Yes

The temperature of all nodes at this
x-location are stored

$\bar{T}_1$, $\bar{q}_1$, $T_{fb}$, $h_x$ and $Nu_x$ are calculated.
The integrations involved are done by
calling subroutine 'SIMPSN'

Is
$k \leq N$?
N is a large number,
suitably chosen such
that $Nu_x$ becomes
almost constant
— No → $k \leftarrow k+1$

Yes

( STOP )

FIG. 4    FLOW CHART OF THE
MAIN PROGRAM.

# CHAPTER 4

## RESULTS AND DISCUSSIONS

Figure 5 shows the temperature distribution in the tube wall for different conductivities of the tube material at the circumferential location, $\emptyset = 0°$ (highest point on the tube). The temperatures in the tube wall and also the temperature gradient are higher for low conductivity material than for high conductivity material. This is because for low conductivity material the resistance to heat transfer is high and hence higher temperature-gradient. Also, because of less heat transfer to the fluid, the inner wall is cooled less by the flowing fluid which results in raising the temperature of the wall. This suggests that in case of low conductivity tube material there is a chance of burn out of the tube at the point of highest temperature which in turn results in leakage of the fluid.

In Figure 6, the effect of wall thickness on the temperature distribution in the tube wall is depicted. It is observed that with the decrease of tube thickness, the temperature gradient decreases and the temperature level in the tube increases. So, a thin tube with low conductivity is not desirable as it may give rise to hot spots occurring due to high temperatures on the surface of the tube. The nature of the curves satisfy the physics as with the reduction of thickness, the thermal resistance to heat flow decreases and hence

FIG. 5  RADIAL VARIATION OF THE TEMPERATURE IN THE TUBE WALL FOR VARIOUS CONDUCTIVITIES OF THE TUBE MATERIAL AT $\phi = 0°$

$( d = 0.1 , Th = 0.02 , W = 1.0 , Pr = 51 , Re = 2000 )$
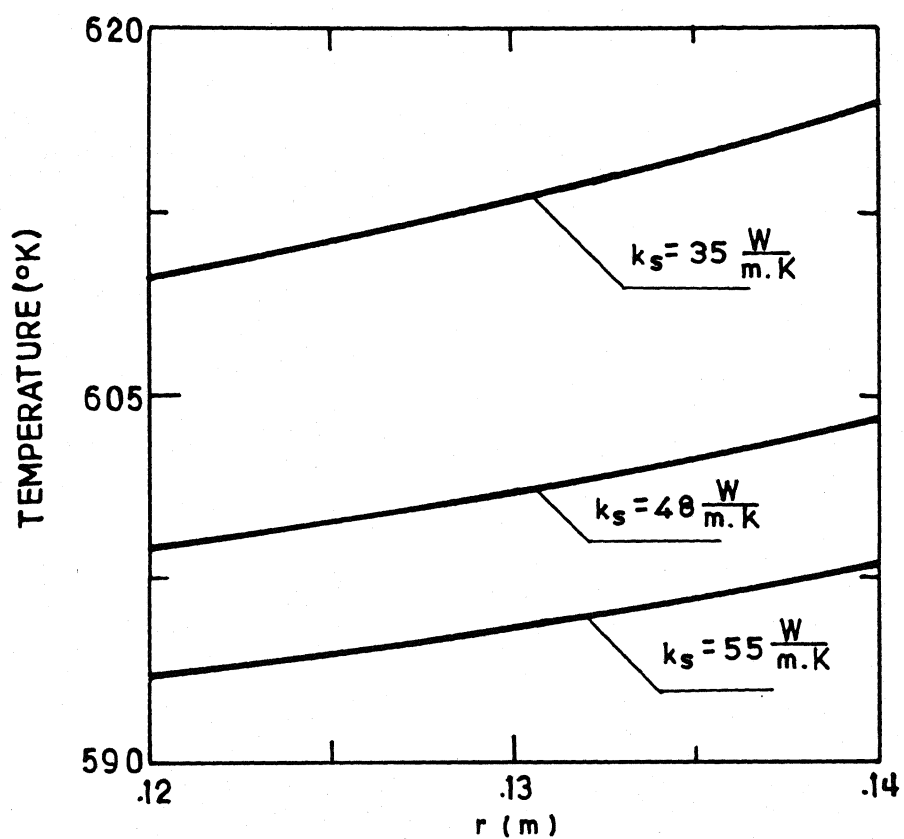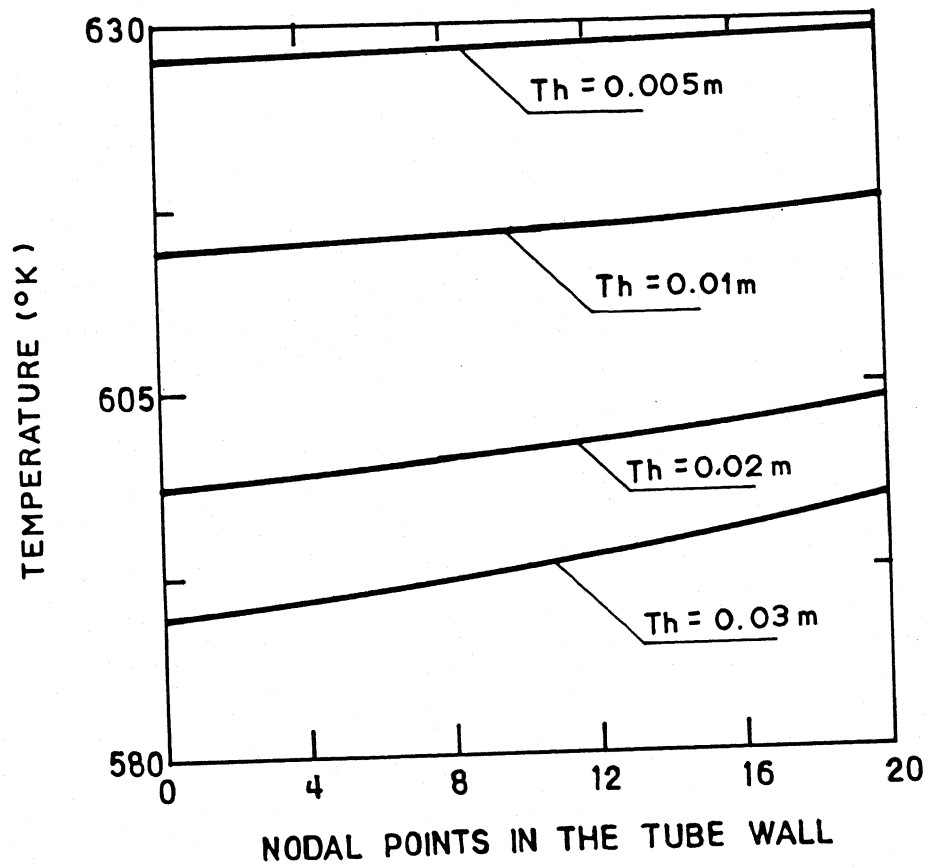
FIG.6 TEMPERATURE VARIATION IN THE TUBE WALL FOR DIFFERENT THICKNESS OF THE TUBE AT $\phi = 0°$ ( d = 0.1 , W =1.0 , $k_s$ = 48 , Pr = 51 , Re = 2000 )

decreases in temperature gradient. Also most of the radiation heat input is used to raise the temperature.

Figure 7 shows the effect of vertical location (d) of the tube with respect to the heated wall on the temperature distribution in the tube wall. As expected, the temperature level shoots up when the tube is placed closer to the wall as it receives more heat from the wall. However, the temperature gradient remains independent of the location of the tube (d) as the tube thickness and thermal conductivity are same for all these cases.

Figure 8 shows the circumferential inner tube wall temperature distribution (fluid-solid interface temperature) at a particular x-location for different widths (W) of the heated wall when the tube is placed equidistant from the two edges of the wall. As one would expect, the curves show symmetric nature about $\emptyset = 180°$ as the radiation heat flux between $0°$ and $180°$ is same as that between $180°$ and $360°$. However, the curve for bigger width of the wall is placed above that for smaller widths of the wall. Also it is more flattened. This is quite expected, as the tube receives more radiation when the heated wall is more wide. The flattened nature is because the circumferential radiation heat flux is more uniform in nature in case of larger width (W) of the heated wall.

Figure 9 indicates the plots of mean inner wall temperature against the axial distance (x) for different Prandtl number fluids, for a constant Reynolds number. It is observed that the mean wall temperature is lower for higher
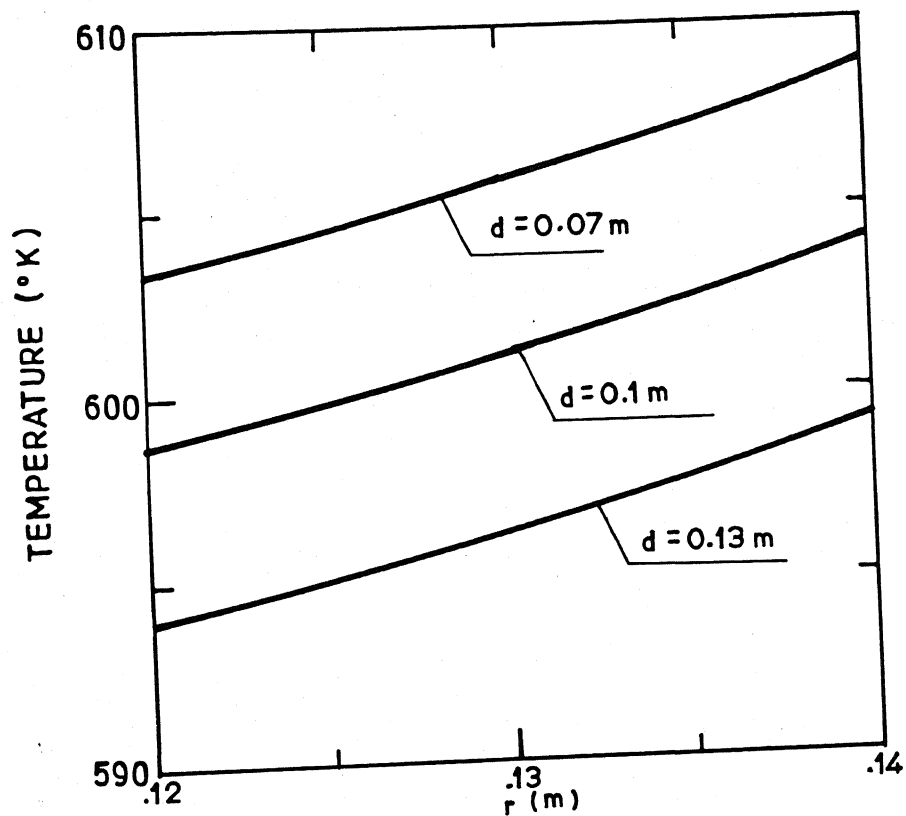
FIG. 7   RADIAL TEMPERATURE DISTRIBUTION IN THE TUBE WALL FOR DIFFERENT VERTICAL POSITION OF THE TUBE (d) WITH RESPECT TO THE HEATED WALL (Th = 0.02 , W = 1.0 , $k_s$ = 48 , Pr = 51 , Re = 2000 )
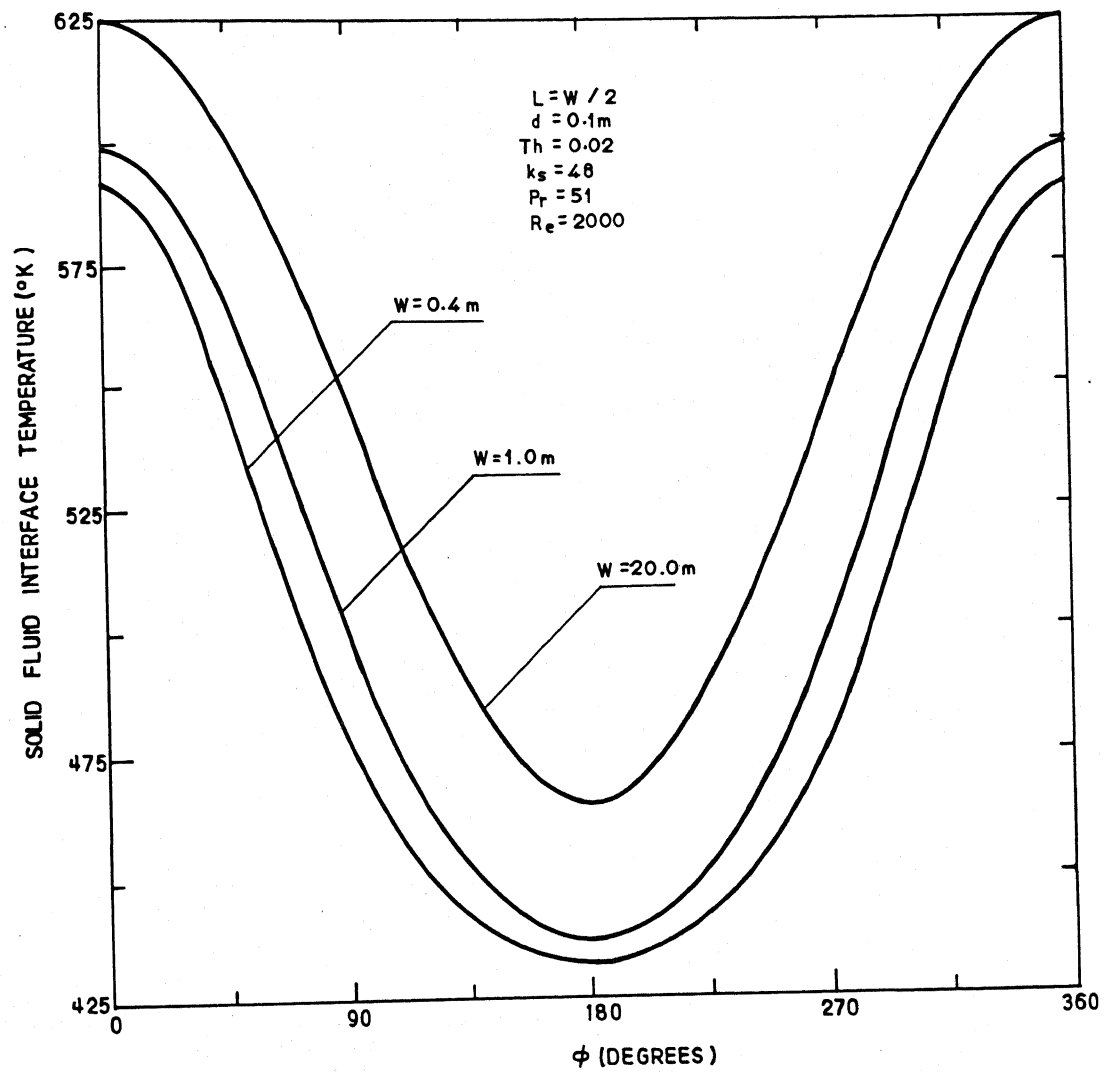
FIG. 8  CIRCUMFERENTIAL VARIATION OF THE FLUID-SOLID INTERFACE TEMPERATURE FOR DIFFERENT WIDTHS OF THE HEATED WALL, AT x = 0.1 m
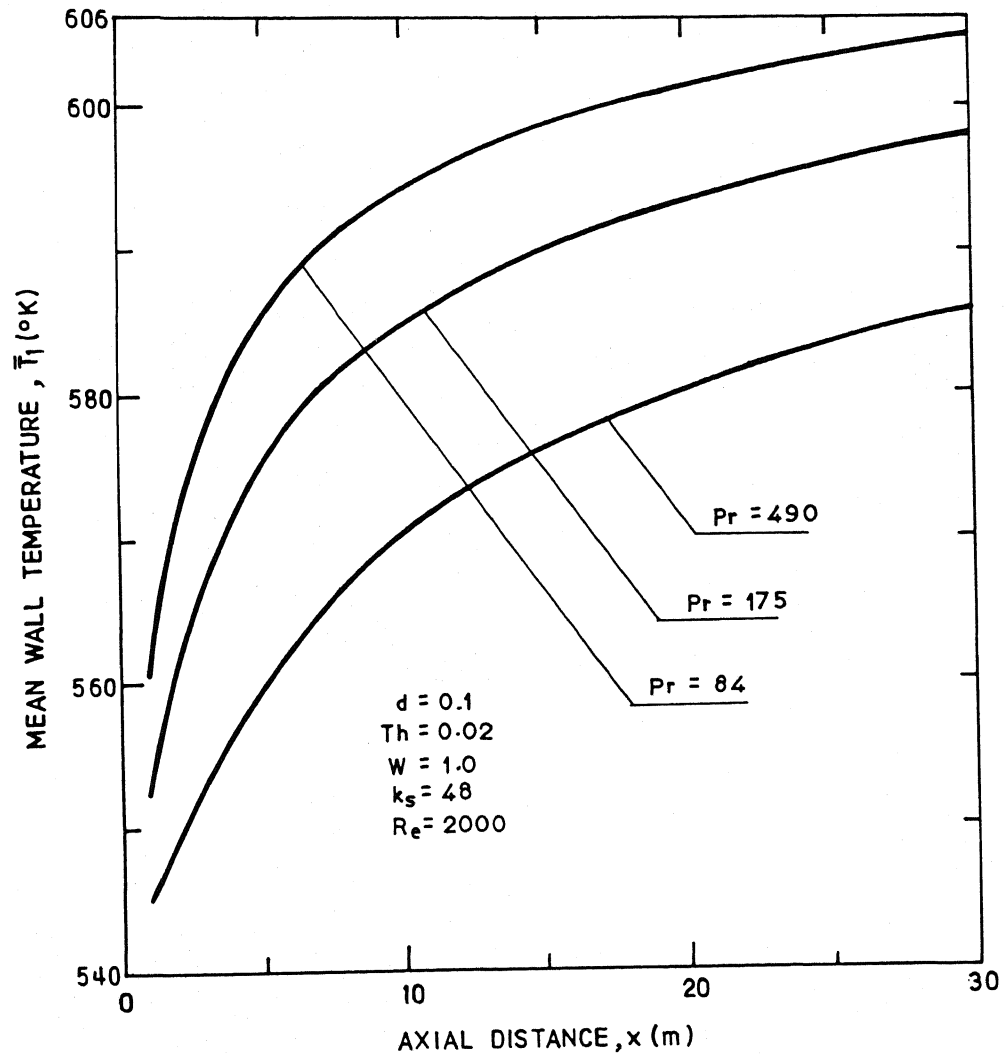
FIG.9  AXIAL DISTRIBUTION OF MEAN WALL TEMPERATURE FOR DIFFERENT PRANDTL NUMBER (Pr) AT A CONSTANT REYNOLDS NUMBER

Prandtl number fluid and the temperature gradient near the entrance of the tube is more in case of low Prandtl number fluid. This is because for low Prandtl number fluid, the thermal diffusion is much more as compared with high Prandtl number fluids. But, as the axial distance increases i.e. at larger x, the temperature gradient is not affected much by Prandtl number as the boundary layer thickness grows along the x-direction.

Figure 10 shows the local Nusselt number, $Nu_x$, variation along the axial distance, x for various Prandtl number fluids, Reynolds number remaining same. As expected, Nusselt number is very high at the entrance of the tube and then it decreases monotonically along x until it becomes almost constant far downstream. Local Nusselt numbers are less for lower Prandtl number fluids. This is because lower Prandtl number fluid have higher thermal diffusivity and hence convective heat transfer is less. So, the heat transfer coefficient is also less which in turn implies that Nusselt number is less. Also, it is seen that thermal entry lengths for higher Prandtl number fluids are much more as they have lower thermal diffusivity which means that thermal boundary layer develops slower.

Figure 11 shows how local Nusselt number, $Nu_x$ changes along 'x' for various Reynolds number, Prandtl number remaining same. For higher Reynolds number of the flow, Nusselt numbers are larger. This is because, higher Reynolds number means higher average velocity of the flow and hence more heat is carried away by the fluid and since Nusselt number is the
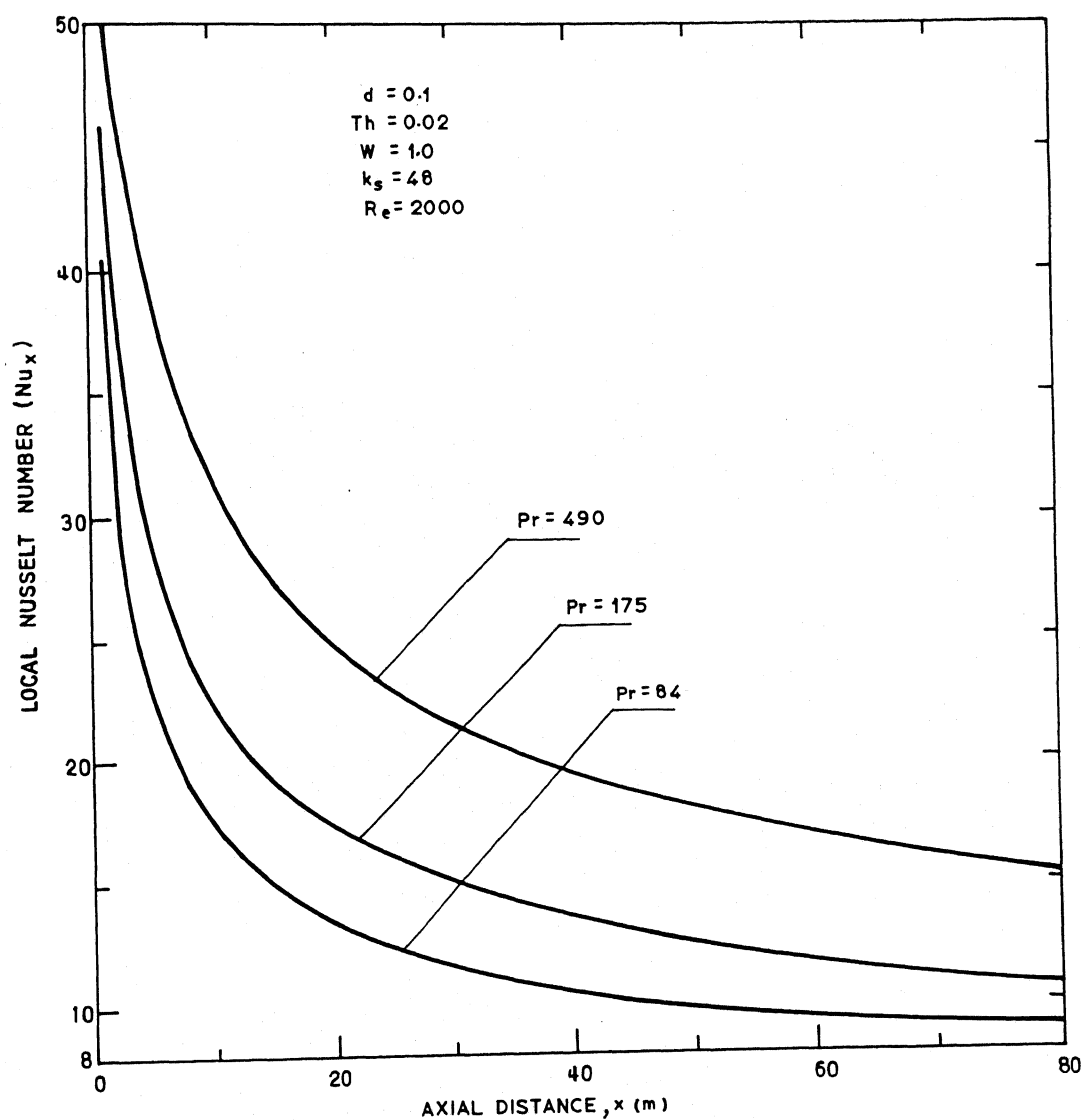
FIG. 10   AXIAL DISTRIBUTION OF LOCAL NUSSELT NUMBER FOR VARIOUS
PRANDTL NUMBER (Pr) AT CONSTANT Re
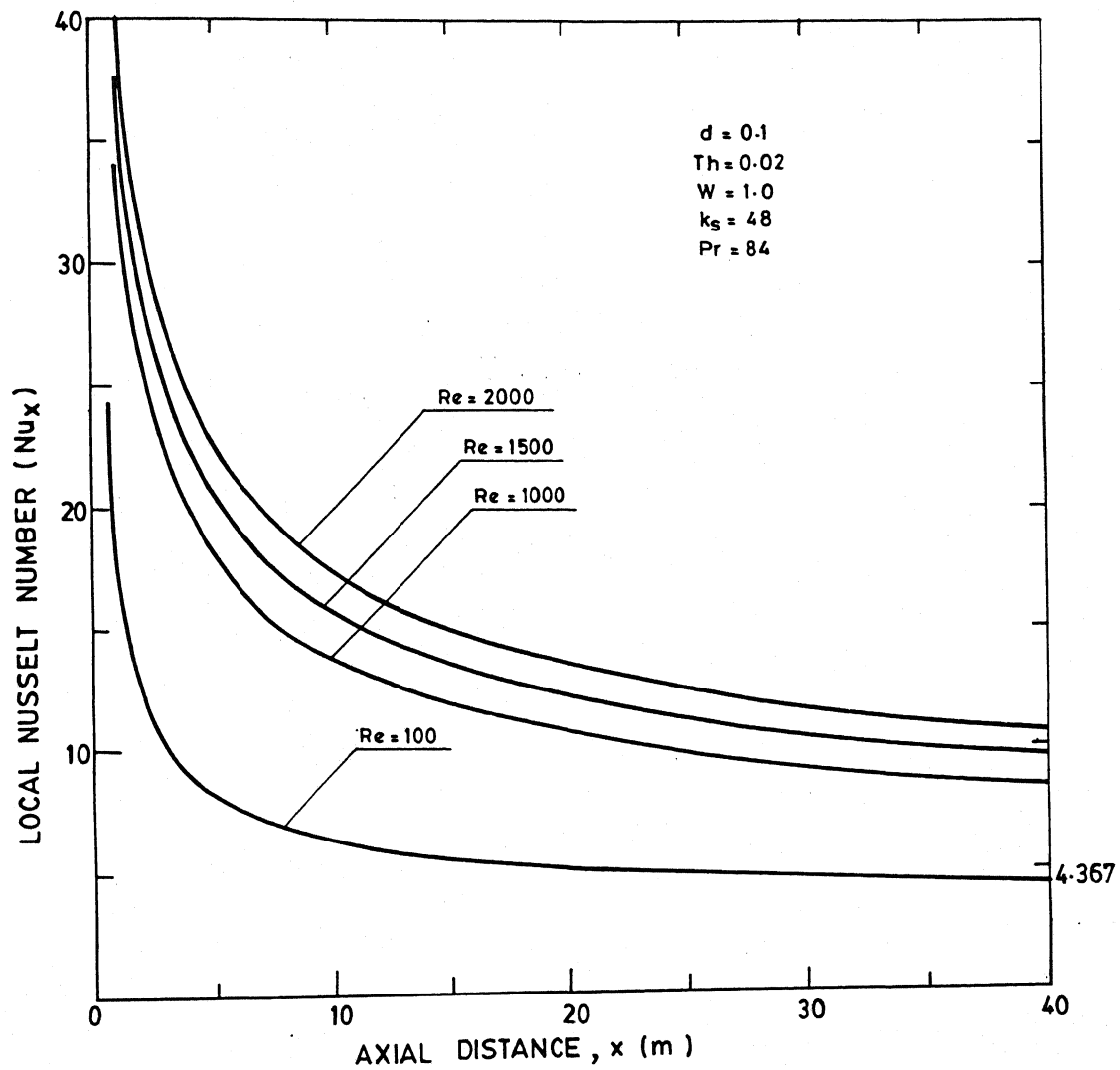
FIG.11    AXIAL DISTRIBUTION OF THE LOCAL NUSSELT NUMBER FOR DIFFERENT REYNOLDS NUMBER (Re ) OF THE FLOW, AT A FIXED VALUE OF Pr

Figure 12 shows plots of fluid bulk temperature $(T_{fb})$ along the axial distance $(x)$ for various Reynolds numbers, Prandtl number remaining same. The plots indicates that fluid bulk temperature increases with the axial distance, x. For higher Reynolds number of the flow, the fluid bulk temperatures are less than that for lower Reynolds number. This is because for higher Reynolds number, the average velocity of the flow is higher which results in more convective heat transfer giving rise to lower bulk temperature of the fluid at a given x-location.

Figure 13 shows plots of fluid bulk temperature $(T_{fb})$ along the axial distance $(x)$ for various Prandtl number fluids, Reynolds number of flow remaining same. The plots indicate that fluid bulk temperature increases with axial distance, x. Also, for higher Prandtl number, fluid bulk temperatures are lower. This is because for higher Prandtl number fluids thermal diffusivity is lower which in turn results in higher convective heat transfer and hence lower fluid bulk temperature at a given x-location.

Finally, the accuracy of the present numerical solution is checked by comparing the Nusselt number for the fully developed condition when constant heat flux condition is imposed on the periphery of the tube and conduction in the tube wall is neglected, i.e. the tube is considered very very thin. Nusselt number at a distance of 2000 meters along the tube is found to be 4.5 which compares very well with 4.364, the Nusselt number for fully developed constant heat flux
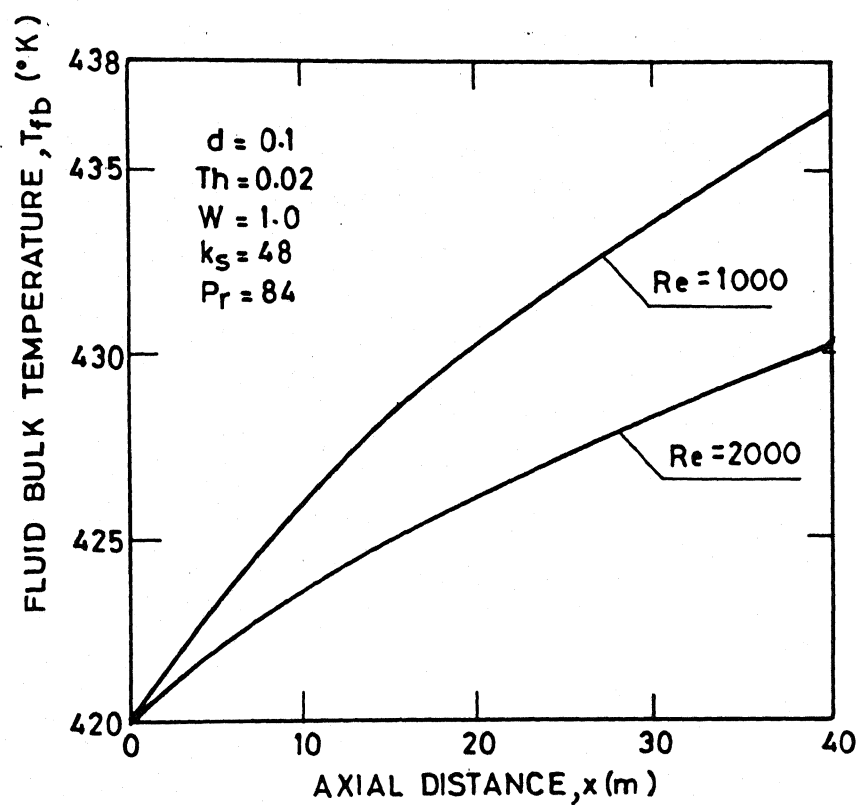
FIG.12  AXIAL DISTRIBUTION OF FLUID BULK TEMPERA-
TURE FOR VARIOUS VALUES OF Re OF THE FLOW
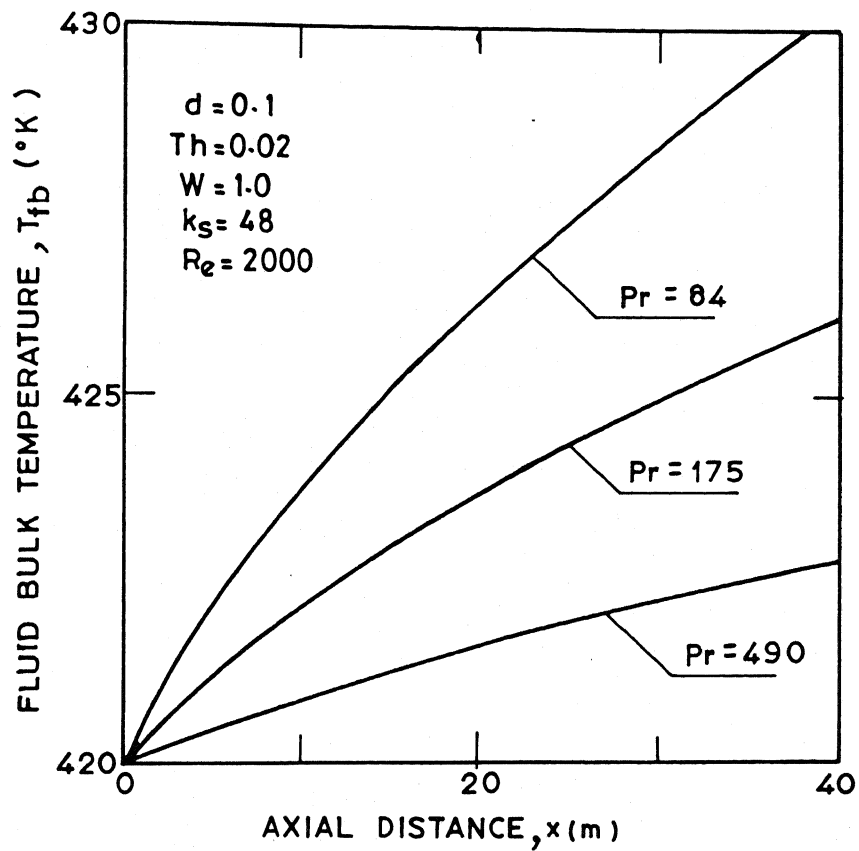
FIG. 13  AXIAL DISTRIBUTION OF THE FLUID BULK TEMPERA-
TURE FOR DIFFERENT VALUES OF PRANDTAL NUMBER
( Pr )

condition as obtained by analytical solution. Since, theoretically thermally fully developed condition occurs at infinity, it is not numerically possible to go to that extent because of limits on computation time. As the local Nusselt number for uniform heat flux condition obtained numerically is very much closer to the value obtained by analytical solution, the present solution for non-uniform heat flux condition can be called accurate enough.

# CHAPTER 5

## CONCLUSIONS

A simple but computationally efficient numerical scheme has been used to solve the problem of conjugate heat transfer in a laminar flow of high Prandtl number fluid in a circular tube whose periphery is exposed to non-uniform radiation heat flux from a large heated wall. The numerical results obtained agree very well with the physical expectations. Also, the accuracy of the present numerical solution has been checked by comparing the Nusselt number obtained numerically for thermally fully developed condition with that obtained analytically for the idealised case of constant heat flux condition on the periphery of a very thin tube. Also, this analysis can be modified to take into account variable property fluid and the tube wall. The present analysis is for infinite length of the tube, but it can also be extended to the tube of finite length with necessary change in boundary conditions.

## REFERENCES

1. Reynolds, W.C., "Heat Transfer to Fully Developed Laminar Flow in a Circular Tube with Arbitrary Circumferential Heat Flux", Trans. ASME, Vol. 82, 1960, pp. 108-112.

2. Reynolds, W.C., "Turbulent Heat Transfer in a Circular Tube with Variable Circumferential Heat Flux", International Journal of Heat and Mass Transfer, Vol. 6, 1963, pp. 445-454.

3. Faghri, M. and Sparrow, E.M., "Simultaneous Wall and Fluid Axial Conduction in Laminar Pipe-Flow Heat Transfer", ASME Journal of Heat Transfer, Vol. 102, 1980, pp. 58-63.

4. Zariffch, E.K., Soliman, H.M. and Trupp, A.C., "The Combined Effects of Wall and Fluid Axial Conduction on Laminar Heat Transfer in Circular Tubes", Paper FC-23, Proceedings, Seventh International Heat Transfer Conference, Vol. IV, 1982, pp. 131-136.

5. Campo, A. and Rangel, R., "Lumped-System Analysis for the Simultaneous Wall and Fluid Axial Conduction in Laminar Pipe-Flow Heat Transfer", Physico Chemical Hydrodynamics, Vol. 4, 1983, pp. 163-173.

6. Davis, E.J. and Venkatesh, S., "The Solution of Conjugated Multiphase Heat and Mass Transfer Problems", Chemical Engineering Science, Vol. 34, 1979, pp. 775-787.

7. Luikov, A.V., Aleksashenko, V.A. and Aleksashenko, A.A., "Analytical Methods of Solution on Conjugated Problems in Convective Heat Transfer", International Journal of Heat and Mass Transfer, Vol. 14, 1971, pp. 1047-1056.

8. Patankar, S.V., "A Numerical Method for Conduction in Composite Materials, Flow in Irregular Geometries and Conjugate Heat Transfer", Paper CO-14, Proceedings, Sixth International Heat Transfer Conference, Vol. III, 1978, pp. 297-302.

9. Barozzi, G.S. and Pagiliarini, G., "A Method to Solve Conjugate Heat Transfer Problems: The Case of Fully Developed Laminar Flow in a Pipe", ASME Journal of Heat Transfer, Vol. 107, 1985, pp. 77-83.

10. Patankar, S.V., Numerical Heat Transfer and Fluid Flow, Hemisphere, Washington, D.C., 1980.

11. Siegel, R. and Howell, J.R., Thermal Radiation Heat Transfer, International Student Edition, McGraw-Hill, 1972.

APPENDIX A

DETERMINATION OF THE CONFIGURATION FACTOR

A.1 Definition

The configuration factor is also called the geometric view factor. For any two given surfaces, the orientation between them affects the fraction of the radiation energy leaving one surface that strikes the other surface directly. Therefore, the orientation of the surfaces plays an important role in radiation heat exchange. The physical significance of the view factor between two surfaces is that it represents the fraction of radiative energy leaving one surface that strikes the other surface directly.

A.2 Hottel's Cross-String Method [11]

Consider an enclosure, as shown in Figure A-1, consisting of four surfaces which are very long in the direction perpendicular to the plane of the figure. The surfaces can be flat, convex or concave. To find the view factor, $F_{1-2}$, imaginary strings are assumed, shown by dashed line in the figure, they are tightly stretched among the four corners A, B, C, D of the enclosure. If $L_i$ (i = 1,2,3,4,5,6) denote the lengths of the strings joining the corners, as illustrated in Figure A-1. According to Hottel, the view factor $F_{1-2}$ can be expressed as,
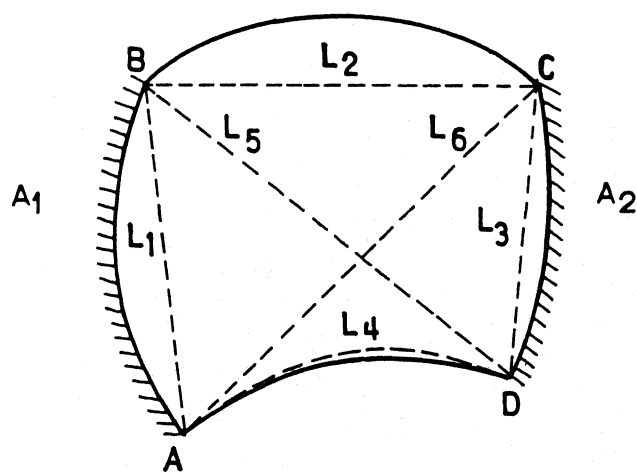
FIG. A-1   DETERMINATION OF CONFIGURATION FACTOR
BETWEEN THE SURFACES $A_1$ AND $A_2$ BY
HOTTEL'S CROSS-STRING METHOD

$$F_{1-2} = \frac{\text{Total crossed length} - \text{Total uncrossed length}}{2 \times \text{Length of surface '1'}}$$

$$= \frac{(L_5 + L_6) - (L_2 + L_4)}{2L_1} \quad , \quad \begin{array}{l}\text{Length of surface '1'}\\ \text{approximated to } L_1\end{array}$$

## A.3  Derivation of the Equations for Determining Configuration Factor

For the present case the configuration factor is found between any point of the outer surface of the tube and the large heated wall placed over the tube. Each point on the upper surface of the tube receives radiation heat flux from the entire plate.

Figure A-2 is considered, the tube is placed at a distance d vertically below the large wall. Both the wall and the tube are infinitely long in the direction perpendicular to the plane of the paper.

In Figure A-2, A is point of tangent on the outer circle from the right end point N, of the wall. Similarly A' is the touching point of the tangent drawn on the outer circle from the left end point, N', of the wall.

Clearly the region below the points A and A' do not get any radiation heat flux directly from the hot plate. Thereby the configuration factor in this region is obviously zero. So, the location of points A and A' is most important, however it is to be noted that when the tube is placed vertically below any edge then point A or A' will be shifted to point C or C' respectively. Therefore in the Figure A-2 angle $\alpha$ cannot be less than $\beta$ and limiting value of $\alpha$ is $\beta$,
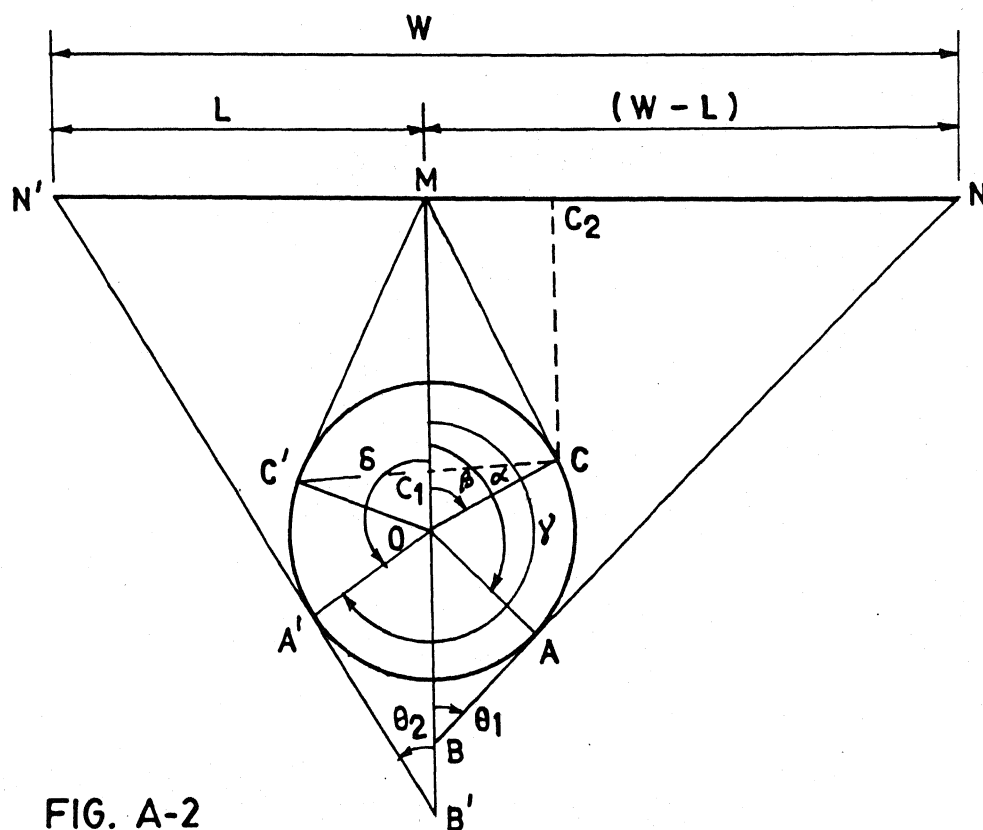
FIG. A-2

however if the top point of the tube, P is placed not directly below the plate then $\alpha$ can be less than $\beta$.

To find out $\beta$ the triangle MCO is considered,

$$MO = d + r_2$$

$$OC = r_2 = \text{Outer radius}$$

$$\therefore \quad MC = \sqrt{OM^2 - OC^2}, \quad \text{as MCO is a right angle triangle and}$$

$$\angle MCO = 90°$$

$$\text{or} \quad MC = \sqrt{(d + r_2)^2 - r_2^2} = \sqrt{d^2 + 2d\ r_2}$$

$$\text{As,} \quad \angle MOC = \beta, \quad \therefore \quad \tan \beta = \frac{MC}{OC} = \frac{\sqrt{d^2 + 2d\ r_2}}{d}$$

$$\therefore \quad \beta = \tan^{-1}\left(\frac{\sqrt{d^2 + 2d\ r_2}}{d}\right) \qquad (A.1)$$

Consider the triangle OAB,

$$\angle AOB = (180° - \alpha)$$

$$\angle OAB = 90°$$

$$\therefore \quad \theta_1 = 180° - [\angle AOB + \angle OAB] = \alpha - 90°$$

In the right angle triangle OAB

$$\frac{OA}{OB} = \sin \theta_1 = \sin(\alpha - 90°) = -\cos\alpha$$

$$\therefore \quad OB = -OA/\cos\alpha = -r_2/\cos\alpha$$

$$\therefore \quad MB = MO + OB = d + r_2 - r_2 \sec\alpha$$

$$MN = W - L$$

$\therefore \quad \dfrac{MN}{MB} = \tan \Theta_1 = \tan(\alpha - 90°) = -\cot\alpha$

or, $\quad \dfrac{W - L}{d + r_2 - r_2 \sec\alpha} = -\cot\alpha$

or, $\quad (W - L)\sin\alpha = -(d + r_2)\cos\alpha + r_2$

Squaring both sides of the above expression and simplifying it the following expression is obtained

$A \cos^2\alpha - B\cos\alpha + C = 0$

where $\quad A = (W - L)^2 + (d + r_2)^2$

$\qquad B = 2r_2(d + r_2)$

$\qquad C = r_2^2 - (W - L)^2$

$\therefore \quad \cos\alpha = \dfrac{B \pm \sqrt{B^2 - 4AC}}{2A}$

$\qquad\qquad = \dfrac{B \pm D}{2A}, \quad D = \sqrt{B^2 - 4AC}$

$\quad \sin\alpha = \sqrt{1 - \cos^2\alpha} = \dfrac{1}{2A}\sqrt{4A^2 - (B + D)^2}$

$\qquad\qquad\qquad\qquad$ when, $\cos\alpha = \dfrac{B + D}{2A}$

$\qquad\qquad = \dfrac{1}{2A}\sqrt{4A^2 - (B - D)^2}$

$\qquad\qquad\qquad\qquad$ when, $\cos\alpha = \dfrac{B - D}{2A}$

$\therefore \quad \tan\alpha = \dfrac{\sqrt{4A^2 - (B - D)^2}}{B - D}$ $\qquad\qquad$ (A.2)

or, $\qquad = \dfrac{\sqrt{4A^2 - (B + D)^2}}{B + D}$

Similarly, to find out $\delta$, the triangle OA'B' is considered.

In triangle OA'B',

$$\angle OB'A' = \theta_2, \qquad \angle B'OA' = (180° - \delta)$$

$$\therefore \quad \theta_2 = 180° - [90° + (180° - \delta)] = (\delta - 90°)$$

$$OB' = OA'/\sin \theta_1 = - r_2/\cos \delta$$

From triangle, MB'N',

$$MB' = MO + OB' = d + r_2 - r_2 \sec \delta$$

$$MN' = L$$

$$\tan \theta_2 = \frac{MN'}{MB'} = \frac{L}{(d + r_2 - r_2 \sec \delta)}$$

or, $\quad -\cot \delta = \dfrac{L}{d + r_2 - r_2 \sec \delta}$

Solving this equation for '$\delta$',

$$\tan \delta = \frac{\sqrt{4A_1^2 - (B_1 + D_1)^2}}{B_1 + D_1} \qquad\qquad (A.3)$$

or, $\qquad = \dfrac{\sqrt{4A_1^2 - (B_1 - D_1)^2}}{B_1 - D_1}$

where, $\quad D_1 = \sqrt{(B_1^2 - 4A_1 C_1)}$

$$A_1 = L^2 + (d + r_2)^2$$

$$B_1 = 2r_2(d + r_2)$$

$$C_1 = r_2^2 - L^2$$

Also, $\quad \gamma = 2\pi - \delta \qquad\qquad (A.4)$

From the equations (A.1), (A.2), (A.3), (A.4) the values of $\beta$, $\alpha$, $\delta$ and $\gamma$ are obtained, which play important role for the calculation of configuration factor.

Next step is to express the configuration factor, $F_{2W}$ as a function of '$\emptyset$'. Refer to Figure A-3.

Let, the configuration factor for the elemental arc XY on the upper surface is required to be found. The length XY is sufficiently small such that in the limiting case this element turns to a point and the expression for $F_{2W}$ for this element becomes the value of $F_{2W}$ at the point P.

Points X and Y are joined with points M and N by four strings, two crossed, two uncrossed, as illustrated in the Figure A-3. Here, XN and YN' are the uncrossed strings and XN' and YN are the crossed strings.

By Hottel's Cross-String method, as described earlier,

$$F_{2W} \text{ at } P = \lim_{XY \to 0} \frac{(XN' + YN) - (XN + YN')}{2XY}$$

$$= \lim_{XY \to 0} \frac{(XN' - YN') + (YN - XN)}{2XY}$$

From the Figure A-3, $\quad XN' - YN' = XY$

and $\quad YN - XN \cong YZ$

where XZ is the perpendicular drawn on YN from X

$$F_{2W} \text{ at } P = \lim_{XY \to 0} \frac{XY + YZ}{2XY}$$

This equation is valid for the right half of the tube, moreover upto $\emptyset = \alpha$.
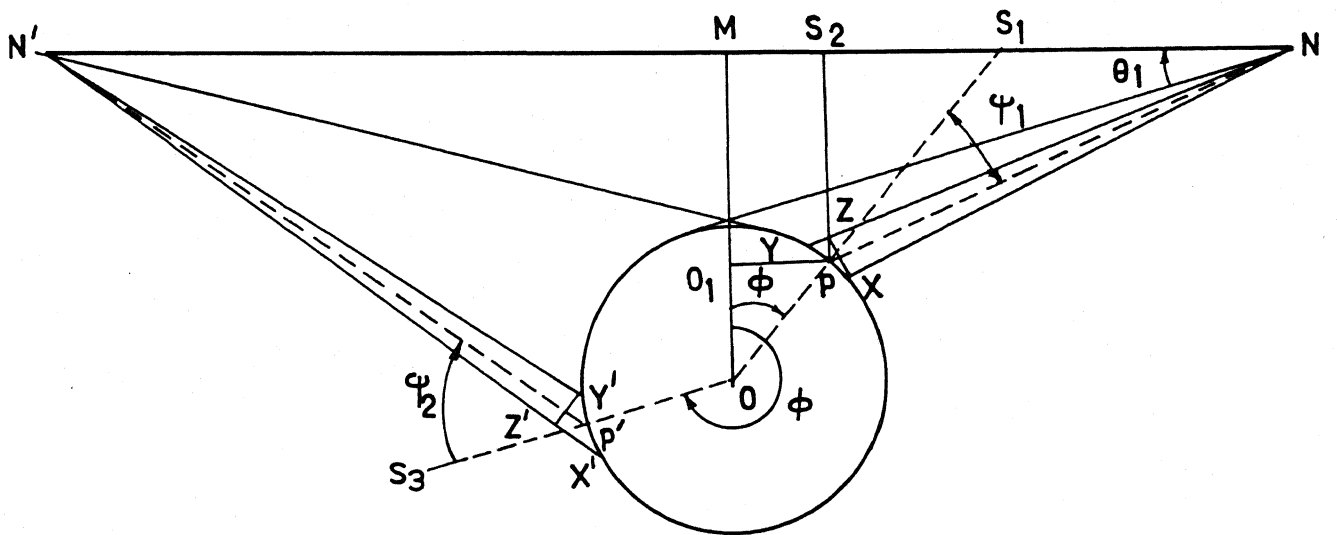
FIG. A-3

For $\emptyset > \alpha$, $F_{2W} = 0$, till $\emptyset = \gamma$ in the other half. To find out YZ, the enlarged view of the triangle XYZ is considered, as shown in Figure A-4.

From this figure, $\angle NPS_1 = \Psi_1$, $\angle YPO = 90°$ as $OS_1$ is normal to the surface at point P.

XY is very small, so that YN and PN are almost parallel, and as XZ is perpendicular to YN, so XZ is also perpendicular to PN, i.e. $\angle PX_1X = 90°$ in the triangle $PX_1X$ and as $OS_1$ is perpendicular to XY, $\angle XPS_1 = 90°$.

$\therefore$ $\angle NPX = 90° - \Psi_1$

$\therefore$ $\angle X_1XP = 180° - [\angle NPX + \angle PX_1X] = \Psi_1$

Now from the right angle triangle YZX,

$$\frac{YZ}{XY} = \sin \Psi_1, \quad \text{i.e. } YZ = XY \sin \Psi_1$$

So, $F_{2W}$ at P or $F_{2W}(\emptyset) = \underset{XY \to 0}{Lt} \frac{XY + YZ}{2XY} = \underset{XY \to 0}{Lt} \frac{XY + XY \sin \Psi_1}{2XY}$

$$= \frac{1}{2}(1 + \sin \Psi_1)$$

$\therefore$ $F_{2W}(\emptyset) = \frac{1}{2}(1 + \sin \Psi_1)$, for $0 \leq \emptyset \leq \alpha$ \hspace{1cm} (A.5)

$\Psi_1$ is found out considering Figure A-4,

From triangle $PS_1N$, $\quad \Psi_1 = \pi - (\Theta_1 + \pi/2 + \emptyset)$

$$= \frac{\pi}{2} - (\Theta_1 + \emptyset) \hspace{1cm} \text{(A.6)}$$

From triangle $PS_2N$, $\quad \tan \Theta_1 = \frac{PS_2}{S_2N}$

$OM = d + r_2$, $MS_2 = r_2 \sin\emptyset$, $MN = (W - L)$,

$OO_1 = r_2 \cos\emptyset$, $S_2N = MN - MS_2 = (W - L) - r_2 \sin\emptyset$
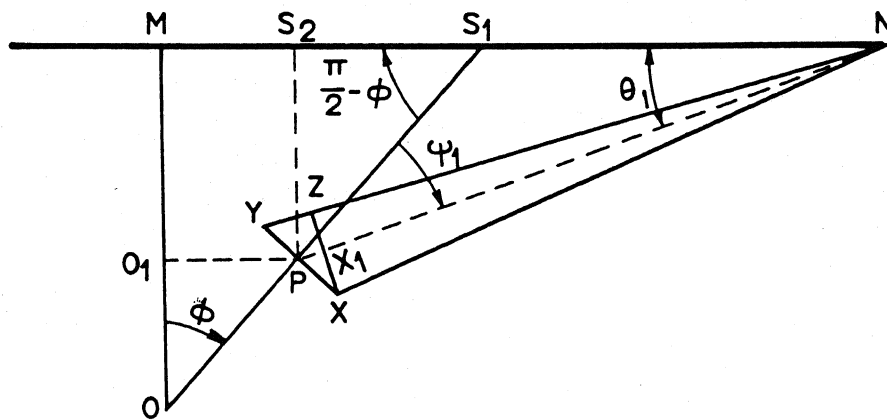
FIG. A-4
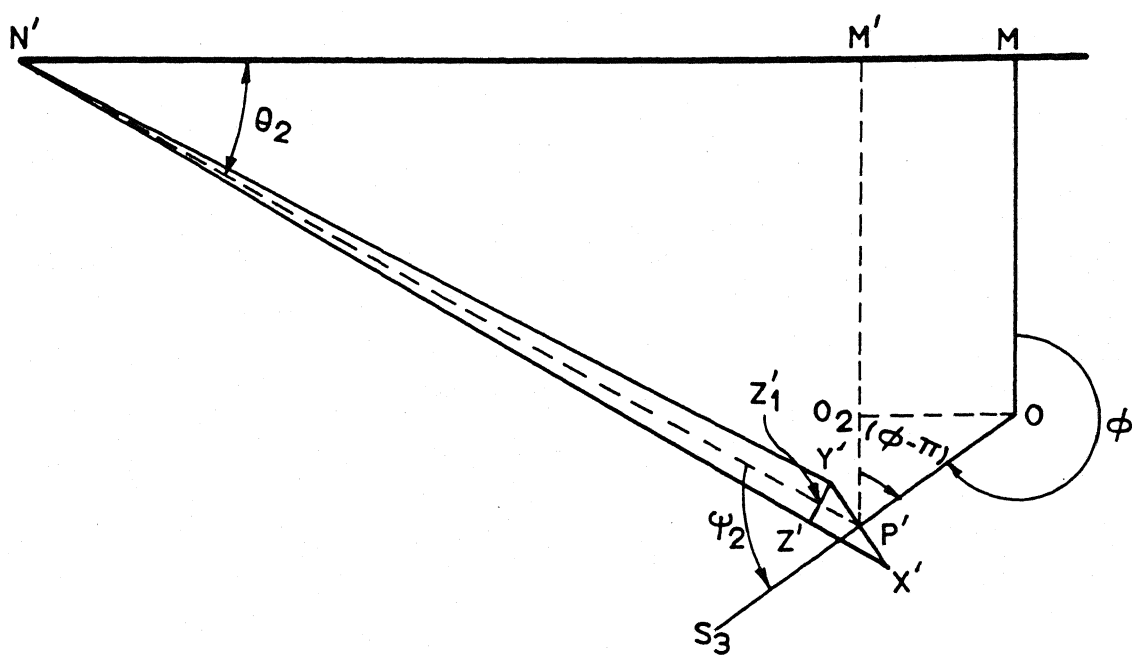
FIG. A-5

From expression of $F_{2W}$ at P',

$$F_{2W} \text{ at P'} = \lim_{X'Y' \to 0} \frac{X'Y' - X'Y' \sin \Psi_2}{X'Y'}$$

or, $F_{2W}$ at P' $= F_{2W}(\phi) = \frac{1}{2}(1 - \sin \Psi_2)$       (A.8)

From the same figure, $\angle OP'O_2 = (\phi - \pi)$

$$M'P'N' = \angle OP'N' - \angle OP'O_2$$

$$= (\pi - \Psi_2) - (\phi - \pi) = 2\pi - (\phi + \Psi_2)$$

From triangle N'M'P', $M'P'N' = \frac{\pi}{2} - \Theta_2$

Equating these two,

$$2\pi - (\phi + \Psi_2) = \frac{\pi}{2} - \Theta_2$$

or, $\Psi_2 = 1.5\pi + \Theta_2 - \phi$       (A.9)

where, $\Theta_2 = \tan^{-1} \frac{P'M'}{M'N'}$

$$P'M' = M'O_2 + O_2P' = d + r_2 + r_2 \cos(\phi - \pi)$$

$$= d + r_2 - r_2 \cos\phi$$

$$M'N' = MN' - MM' = L - r_2 \sin(\phi - \pi) = L + r_2 \sin\phi$$

$$\Theta_2 = \tan^{-1}\left(\frac{d + r_2 - r_2 \cos\phi}{L + r_2 \sin\phi}\right) \quad\quad\quad (A.10)$$

Therefore all the expressions for $F_{2W}(\phi)$ for different values of $\phi$ are listed below.

$$F_{2W}(\emptyset) = \frac{1}{2}(1 + \sin \Psi_1), \quad \text{for } 0 \leq \emptyset \leq \alpha$$

$$= 0 \quad , \quad \text{for } \alpha < \emptyset < \gamma$$

$$= \frac{1}{2}(1 - \sin \Psi_2), \quad \text{for } \gamma \leq \emptyset \leq 2\pi$$

where

$$\Psi_1 = \frac{\pi}{2} - (\Theta_1 + \emptyset),$$

$$\text{and } \Theta_1 = \tan^{-1} \left[ \frac{(d + r_2) - r_2 \cos\emptyset}{(W - L) - r_2 \sin\emptyset} \right]$$

$$\Psi_2 = 1.5\pi + \Theta_2 - \emptyset,$$

$$\text{and } \Theta_2 = \tan^{-1} \left[ \frac{(d + r_2) - r_2 \cos\emptyset}{L + r_2 \sin\emptyset} \right]$$

# APPENDIX B

## THE LINE-BY-LINE METHOD

A line-by-line method is a conventional combination of TDMA (Tri-Diagonal Matrix Algorithm) method for one dimensional situations and the Gauss-Seidel iterative method. According to this method a grid line (in a particular direction) is chosen and the values of temperatures, T's (or any dependent variable) along the neighbouring lines are assumed or known by their latest values, and the T's along the chosen line are solved by TDMA. This procedure is followed for all the lines in the same direction and then the technique is repeated till the required convergence is attained. Sometimes to make the convergence faster the same procedure is repeated for the lines in other direction.

To visualize the line-by-line method more clearly the Figure B-1 is considered. The discretization equations for the grid points along a particular line (either in x-direction or in y-direction) are considered. These equations contain the temperatures at the grid points (shown by crosses) along the two neighbouring lines. If these temperatures are substituted from their latest values, the equations for the grid points (shown by dots) along the chosen line would look like one dimensional equations and could be solved by TDMA. This procedure is carried out for all the lines in y-direction and may be followed by a similar treatment for x-direction.
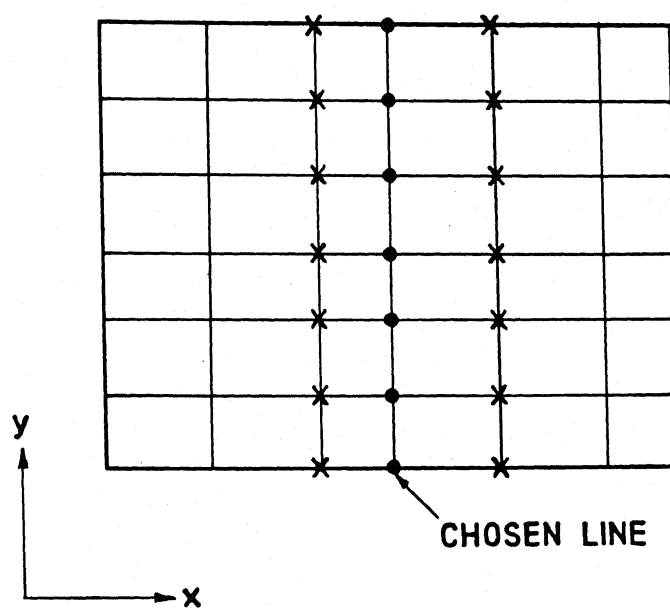
FIG. B-1  REPRESENTATION OF THE LINE-BY-LINE
METHOD

The convergence of the line-by-line method is faster because the boundary condition information from the ends of the line is transmitted at once to the interior of the calculation domain, no matter how many grid points lie along the line. The sweep direction (i.e. the sequence in which lines are chosen) plays an important role in the convergence of the iterative technique. A sweep from upstream to downstream would produce much faster convergence than a sweep against the stream.

# APPENDIX C

## INPUT DATA TO THE PROGRAM

i) Geometry of the tube:

| $r_1$ (m) | $Th = (r_2 - r_1)$, (m) |
|-----------|--------------------------|
| 0.12 | 0.005<br>0.01<br>0.02<br>0.03 |

ii) Position of the tube:

| d (m) | W (m) | L (m) |
|-------|-------|-------|
| 0.07<br>0.10<br>0.13 | 0.4<br>1.0<br>20.0 | $\frac{W}{2}$ |

iii) Conductivity of the tube material, $k_s$ ($\frac{W}{m.K}$):

$k_s = 35$, 48 and 55.

iv) Known temperatures (°K)

$T_e = 420.0$, $T_S = 300.0$, $T_W = 830.0$

v) Radiation parameters:

$\sigma = 0.567 \times 10^{-7}$ W/(m$^2$.K$^4$), $\varepsilon = 0.79$

vi) Flow parameter:

Re = 100, 1000, 1500 and 2000

where,

Re is defined as: $Re = \dfrac{\bar{u} (2r_1)}{\nu}$

vii) Number of grid points taken for numerical solution:

$N_r = 50$, $N_{rf} = 30$, $N_\emptyset = 40$

viii) Properties of fluids:

| Pr | $k_f$ $\frac{W}{m.K}$ | $\alpha$ $\frac{m^2}{s}$ $\times 10^7$ | $\nu$ $\frac{m^2}{s}$ $\times 10^6$ |
|---|---|---|---|
| 51 | 0.260 | 0.932 | 4.75 |
| 84 | 0.132 | 0.663 | 5.60 |
| 175 | 0.135 | 0.710 | 12.40 |
| 490 | 0.138 | 0.769 | 37.50 |

# A P P E N D I X   D

## LISTING  OF  THE  COMPUTER  PROGRAM

### NOMENCLATURE :

| | | | | |
|---|---|---|---|---|
| A | = coefficient of TDM | | NR | $= N_r$ |
| AK | $= k_s$ | | NRF | $= N_{rf}$ |
| AKF | $= k_f$ | | NPR | $= Pr$ |
| AL | $= L$ | | PI | $= \pi$ |
| ALPHA | $= \alpha$ | | QB | $= \bar{q}_f$ |
| ANU | $= Nu$ | | R1 | $= r_1$ |
| ANUF | $= \nu$ | | R2 | $= r_2$ |
| B | = coefficient of TDM | | RENOLD | $= Re$ |
| C | = coefficient of TDM | | RI | $= r_i$ |
| D | = coefficient of TDM | | SIG | $= \sigma$ |
| D4 | $= d$ | | T | $= T$ |
| DPHI | $= \Delta\phi$ | | TFB | $= T_{fb}$ |
| DR | $= \Delta r_s$ | | TFP | $= T_p$ |
| DRF | $= \Delta r_f$ | | TS | $= T_s$ |
| DX | $= \Delta x$ | | TW | $= T_w$ |
| EPS | $= \epsilon$ | | TWB | $= \bar{T}_1$ |
| EPSN | = Accuracy factor for convergence check | | U | $= u$ |
| F2W | $= F_{2w}$ | | UAVER | $= \bar{u}$ |
| H | $= h$ | | V | = final soln. vector of TDMA |
| I | $= i$ | | W | $= W$ |
| J | $= j$ | | | |
| K | $= k$ | | | |

```
C      ********************************************************

C              M. TECH  THESIS

C      TITLE:  C O N J U G A T E   H E A T   T R A N S F E R   I N   A

C      L A M I N A R   P I P E   F L O W   S U B J E C T E D   TO

C      N O N - U N I F O R M   R A D I A T I O N   F R O M   A   L A R G E

C      H E A T E D   W A L L  :  T H E   C A S E   O F   T H E R M A L L Y

C      U N D E V E L O P E D   F L O W


C      ********************************************************


C              M A I N   P R O G R A M


C      ********************************************************
       COMMON/AREA1/D4,R2,AL,W,F2W
       COMMON/AREA2/A,B,C,D,V
       DIMENSION T(50,50),A(50),B(50),C(50),D(50),V(50),F2W(50)
       DIMENSION TFP(50,50),TT1(50),S(50),U(50),RI(50),TWALL(50)
       DIMENSION Q(50)
       OPEN(UNIT=21,DEVICE='DSK',FILE='MASTER.OUT')
       AL=0.5;W=1.0;R1=0.12;R2=0.14;D4=0.1;
       AK=48.0;TS=300.0;SIG=0.567E-07;TW=830.0;EPS=0.79
       AKF=0.132;NRF=30
       NFM1=NRF-1
       ALPHA=0.663E-07
       RENOLD=1500.0;NPR=84;ANUF=0.056E-04
       UAVER=RENOLD*0.5*ANUF/R1
       TYPE *,UAVER
       WRITE(21,3333)NPR,RENOLD,ANUF,UAVER
```

```
3333      FORMAT(2X,I6,2X,F6.1,2X,E8.3,2X,F10.4/)

          DRF=R1/FLOAT(NRF-1)

          PI=3.1415927;NPHI=40;NR=50

          TPI=2.*PI

          DPHI=TPI/FLOAT(NPHI)

          DR=(R2-R1)/FLOAT(NR-NRF)

          P1=2.*R1*DRF+DRF*DRF

          P2=2.*R1*DR-DR*DR

          R=P1*AK/(P2*AKF)

          RR=(R*DR*DR+DRF*DRF)/(DPHI*DPHI)

          A1=2.*R1*R1

          A3=A1*R

          A2=-(A3+A1+2.*RR)

          S2=2.*DR*SIG*EPS/AK

          S2=S2*(2.*R2*R2+R2*DR)

          DX=1.0

          DRDP=DR/DPHI

          DRDPF=DRF/DPHI

          EPSN=0.1

          DO 10 I=1,NRF

          RI(I)=DRF*(I-1)

10        U(I)=1.0-RI(I)*RI(I)/(R1*R1)

          DO 15 I=NRF+1,NR

15        RI(I)=R1+DR*(I-NRF)

          DO 205 I=1,NRF

          DO 205 J=1,NPHI

205       TFP(I,J)=420.0

          CALL CONFIG(1,NPHI)
```

```
        CONST=4.0*DRF*DRF*UAVER/(ALPHA*DX)

        XX=0.0

        DO 202 K=1,50

        DO 40 I=1,NR

        DO 40 J=1,NPHI

40      T(I,J)=450.

        DO99 ITER =1,200

        TOLD=T(NR,1)

C       *************** J=1 ****************

        DO 1651 I=2,NRF-1

        A(I)=2.*RI(I)*RI(I)-RI(I)*DRF

        C(I)=2.*RI(I)*RI(I)+RI(I)*DRF

        B(I)=-4.*RI(I)*RI(I)-4.*DRDPF*DRDPF-CONST*RI(I)*RI(I)*U(I)

1651    D(I)=-CONST*RI(I)*RI(I)*U(I)*TFP(I,1)-2.*DRDPF*DRDPF*(T(I,2)+
        1T(I,NPHI))

        A(1)=0.0

        B(1)=-1.0;C(1)=1.0;D(1)=0.0

        DO101I=NRF+1,NR

        A(I)=2.*RI(I)*RI(I)-RI(I)*DR

        C(I)=2.*RI(I)*RI(I)+DR*RI(I)

        B(I)=-4.*RI(I)*RI(I)-4.*DRDP*DRDP

101     D(I)=-2.*DRDP*DRDP*T(I,NPHI)-2.*DRDP*DRDP*T(I,2)

        A(NR)=4.*R2*R2

        C(NR)=0.0

        B(NR)=B(NR)-4.*S2*T(NR,1)**3.

        D(NR)=D(NR)-S2*F2W(1)*TW**4.-S2*(1.-F2W(1))*TS**4.-3.*S2
        1*T(NR,1)**4.

        A(NRF)=A1;B(NRF)=A2;C(NRF)=A3
```

```
          D(NRF)=-RR*T(NRF,2)-RR*T(NRF,NPHI)

          CALL TRIDAG(1,NR)

          DO 102  I=1,NR

102       T(I,1)=V(I)

C         ********************** J=2,NPHI-1 ***********************

          DO 103 J=2,NPHI-1

          DO 210  I=2,NRF-1

          A(I)=2.*RI(I)*RI(I)-RI(I)*DRF

          C(I)=2.*RI(I)*RI(I)+RI(I)*DRF

          B(I)=-4.*RI(I)*RI(I)-4.*DRDPF*DRDPF-CONST*RI(I)*RI(I)*U(I)

210       D(I)=-CONST*RI(I)*RI(I)*U(I)*TFF(I,J)-2.*DRDPF*DRDPF*(T(I,J+1)+
         1T(I,J-1))

          A(1)=0.0$C(1)=1.0

          B(1)=-1.0$D(1)=0.0

          DO 104 I=NRF+1,NR

          A(I)=2.*RI(I)*RI(I)-RI(I)*DR

          C(I)=2.*RI(I)*RI(I)+RI(I)*DR

          B(I)=-4.*RI(I)*RI(I)-4.*DRDP*DRDP

104       D(I)=-2.*DRDP*DRDP*T(I,J-1)-2.*DRDP*DRDP*T(I,J+1)

          A(NR)=4.*R2*R2

          C(NR)=0.0

          B(NR)=B(NR)-4.*S2*T(NR,J)**3.

          D(NR)=D(NR)-S2*F2W(J)*TW**4.-S2*(1.-F2W(J))*TS**4.-3.*S2
         1*T(NR,J)**4.

          A(NRF)=A1$B(NRF)=A2$C(NRF)=A3

          D(NRF)=-RR*(T(NRF,J+1)+T(NRF,J-1))

          CALL TRIDAG(1,NR)

          DO 105  I=1,NR
```

```
105       T(I,J)=V(I)

103       CONTINUE

C         ********************** J=NPHI ***************************

          DO 215 I=2,NRF-1

          A(I)=2.*RI(I)*RI(I)-RI(I)*DRF

          C(I)=2.*RI(I)*RI(I)+RI(I)*DRF

          B(I)=-4.*RI(I)*RI(I)-4.*DRDPF*DRDPF-CONST*RI(I)*RI(I)*U(I)

215       D(I)=-CONST*RI(I)*RI(I)*U(I)*TFP(I,NPHI)-2.*DRDPF*DRDPF*(T(I,1)
          1+T(I,NPHI-1))

          A(1)=0.0;B(1)=-1.0;C(1)=1.0;D(1)=0.0

          DO 106 I=NRF+1,NR

          A(I)=2.*RI(I)*RI(I)-RI(I)*DR

          C(I)=2.*RI(I)*RI(I)+RI(I)*DR

          B(I)=-4.*RI(I)*RI(I)-4.*DRDP*DRDP

106       D(I)=-2.*DRDP*DRDP*T(I,NPHI-1)-2.*DRDP*DRDP*T(I,1)

          A(NR)=4.*R2*R2

          C(NR)=0.0

          B(NR)=B(NR)-4.*S2*T(NR,NPHI)**3.

          D(NR)=D(NR)-S2*F2W(NPHI)*TW**4.-S2*(1.-F2W(NPHI))*TS**4.-S2*3.*
          1T(NR,NPHI)**4.

          A(NRF)=A1;B(NRF)=A2;C(NRF)=A3

          D(NRF)=-RR*T(NRF,1)-RR*T(NRF,NPHI-1)

          CALL TRIDAG(1,NR)

          DO 107  I=1,NR

107       T(I,NPHI)=V(I)

          IF(ABS(TOLD-T(NR,1)).LE.EPSN)GO TO 110

99        CONTINUE

          WRITE(21,115)
```

```
115       FORMAT(2X,'NOT CONVERGED'//)

          WRITE(21,777)

777       FORMAT(2X,'INTER FACE TEMP. ,J=1,NPHI'//)

          WRITE(21,779)(T(NRF,J),J=1,NPHI)

779       FORMAT(8(F12.3))

          WRITE(21,885)

885       FORMAT(2X,'TEMP. FOR THE WHOLE REGION WITH J=1,NPHI,5&I=1,5'/)

          WRITE(21,*)((T(I,J),J=1,NPHI,5),I=1,NR)

          DO 889 I=1,NRF

          DO 889 J=1,NPHI

889       TFP(I,J)=T(I,J)

C         H E A T   T R A N S F E R   C A L C U L A T I O N S

          DO 11 I=1,NRF

          DO 12 J=1,NPHI

12        TT1(J)=T(I,J)

          TT1(NPHI+1)=TT1(1)

          CALL SIMPSN(0,TPI,NPHI,TT1,XINTGL)

          S(I)=XINTGL*RI(I)*U(I)

11        CONTINUE

171       CALL SIMPSN(0,R1,NFM1,S,XINTGL)

          TFB=2.*XINTGL/(PI*R1*R1)

          DO 13 J=1,NPHI

          TWALL(J)=T(NRF,J)

13        Q(J)=(T(NRF+1,J)-T(NRF,J))/DR

          TWALL(NPHI+1)=TWALL(1)

          Q(NPHI+1)=Q(1)

          CALL SIMPSN(0,TPI,NPHI,TWALL,XINTGL)

          TWB=XINTGL/TPI
```

```
        CALL SIMPSN(O,TPI,NPHI,Q,XINTGL)

        QB=XINTGL/TPI

        H=AK*QB/(TWB-TFB)

        ANU=2.*H*R1/AKF

        TYPE *,ANU

        XX=XX+DX

        WRITE(21,14)XX,TWB,QB,TFB,H,ANU

14      FORMAT(2X,F8.2,4X,F8.3,4X,F7.2,4X,F8.3,4X,F7.3,4X,F8.3)

202     CONTINUE

        STOP

        END


C       ***********************************************************

C                  S U B R O U T I N E : T R I D A G

C       (THIS SUBROUTINE SOLVES SIMULTANEOUS LINEAR NON-HOMOGENIOUS EQNS.

C       BY TRI-DIAGONAL MATRIX SOLUTION)

C       ***********************************************************

        SUBROUTINE TRIDAG(IF,L)

        COMMON/AREA2/A,B,C,D,V

        DIMENSION BETA(51),GAMMA(51)

        DIMENSION A(50),B(50),C(50),D(50),V(50)

C       COMPUTE INTERMEDIATE ARRAYS BETA AND GAMMA

        BETA(IF)=B(IF)

        GAMMA(IF)=D(IF)/BETA(IF)

        IFP1=IF+1

        DO 1 I=IFP1,L

        BETA(I)=B(I)-A(I)*C(I-1)/BETA(I-1)

1       GAMMA(I)=(D(I)-A(I)*GAMMA(I-1))/BETA(I)
```

```
C      COMPUTE FINAL SOLUTION VECTOR V

       V(L)=GAMMA(L)

       LAST=L-IF

       DO 2 K=1,LAST

       I=L-K

2      V(I)=GAMMA(I)-C(I)*V(I+1)/BETA(I)

       RETURN

       END

C      ****************************************************************F

C         S U B R O U T I N E : C O N F I G

C             SUBROUTINE TO CALCULATE CONFIGURATION FACTOR


C      ****************************************************************
       SUBROUTINE CONFIG(IS,NPHI)

       COMMON/AREA1/D4,R2,AL,W,F2W

       DIMENSION F2W(50)

       PI=3.1415927

       TPI=2.*PI

       D1=SQRT(D4*D4+2.*R2*D4)

       BETA=ATAN(D1/R2)

       B1=2.*R2*(D4+R2)

       C1=R2*R2-(W-AL)*(W-AL)

       A1=(D4+R2)*(D4+R2)+(W-AL)*(W-AL)

       D1=SQRT(B1*B1-4.*A1*C1)

       D2=4.*A1*A1-(D1+B1)*(D1+B1)

       D2=SQRT(D2)

       ALPHA1=ATAN(D2/(B1+D1))
```

```
          D2=4.*A1*A1-(D1-B1)*(D1-B1)

          D2=SQRT(D2)

          ALPHA2=ATAN(D2/(B1-D1))

          IF(ALPHA2.LT.0.0)ALPHA2=ALPHA2+PI

          IF(ALPHA2.LT.BETA) GO TO5

          ALPHA=ALPHA2

          GO TO 6

5         ALPHA=ALPHA1

6         C1=R2*R2-AL*AL

          A1=AL*AL+(D4+R2)*(D4+R2)

          D1=SQRT(B1*B1-4.*A1*C1)

          D2=4.*A1*A1-(D1+B1)*(D1+B1)

          D2=SQRT(D2)

          ALPHA1=ATAN(D2/(D1+B1))

          D2=4.*A1*A1-(D1-B1)*(D1-B1)

          D2=SQRT(D2)

          ALPHA2=ATAN(D2/(B1-D1))

          IF(ALPHA2.LT.0.0)ALPHA2=ALPHA2+PI

          IF(ALPHA2.LT.BETA) GO TO 7

          DELTA=ALPHA2

          GO TO 16

7         DELTA=ALPHA1

16        DPHI=TPI/FLOAT(NPHI)

          GAMA=TPI-DELTA

          PHI=0.0

          K=1

10        X=(D4+R2-R2*COS(PHI))/(W-AL-R2*SIN(PHI))

          THETA=ATAN(X)
```

```
        SY1=0.5*PI-THETA-PHI

        F1W=0.5*(1.+SIN(SY1))

        F2W(K)=F1W

        WRITE(21,*)PHI,F1W

        PHI=PHI+DPHI

        K=K+1

        IF(PHI.LE.ALPHA)GO TO 10

15      F1W=0.0

        WRITE(21,*)PHI,F1W

        F2W(K)=F1W

        K=K+1

        PHI=PHI+DPHI

        IF(PHI.LE.GAMA)GO TO 15

20      X=(D4+R2-R2*COS(PHI))/(AL+R2*SIN(PHI))

        THETA=ATAN(X)

        SY1=1.5*PI+THETA-PHI

        F1W=0.5*(1.-SIN(SY1))

        WRITE(21,*)PHI,F1W

        F2W(K)=F1W

        K=K+1

        PHI=PHI+DPHI

        IF(PHI.LE.TPI)GO TO 20

        RETURN

        END

C       ********************************************************************

C       S U B R O U T I N E :  S I M P S N
```

```
C      THIS  SUBPROGRAM INTEGRATES ANY GIVEN FUNCTION OVER A FINITE

C      LIMIT USING SIMPSON'S 1/3-RD RULE

C      ***************************************************************
       SUBROUTINE SIMPSN(XMIN,XMAX,N,DUMMYF,XINTGL)

       DIMENSION DUMMYF(50)

       H=(XMAX-XMIN)/FLOAT(N)

       SUM=0.0

       DO 4 I=2,N

       IF(MOD(I,2))2,2,3

2      SUM=SUM+4.*DUMMYF(I)

       GO TO 4

3      SUM=SUM+2.*DUMMYF(I)

4      CONTINUE

       XINTGL=H/3.*(DUMMYF(1)+SUM+DUMMYF(N+1))

       RETURN

       END


C      ******************* E  N  D  ***************************
```